EVALUATION OF SAFETY PARAMETERS FOR GHARR-1 AFTER NINETEEN (19) YEARS OF OPERATION

This thesis is submitted to the University of Ghana, Legon

By

Bright Madinka Mweetwa

(10444951)

In partial fulfillment of the requirement for the award of

MPhil Nuclear Science and Technology (Nuclear Engineering Option) Degree

July, 2015

DECLARATION

I hereby declare that with the exception of references to other people's work which have been duly acknowledged, this compilation is the result of my own research work and no part of it has been presented for another degree in this University or elsewhere.

……. Date……..…….

(Candidate)

I hereby declare that the preparation of this project was supervised in accordance with the guidelines of the supervision of Thesis work laid down by the University of Ghana.

…… ……..

Dr. E. Ampomah- Amoako **Prof. Emeritus E. H. K. Akaho**

(PRINCIPAL SUPERVISOR) (CO-SUPERVISOR)

Date…… Date……....

DEDICATION

I hereby dedicate this thesis work to my father and mother Mr. Adam and Lilian Mweetwa and above it all to my son Mukomi Mweetwa.

ACKNOWLEDGEMENT

First of all I would like to thank the Almighty God for his protection, provisions, and for making my studies a success. Without him I would literally do nothing. I owe it all to him.

I would like to express my sincere appreciation to my supervisors Dr. E. Ampomah-Amoako, Prof. Emeritus. E. H. K. Akaho, and Mr. H. C. Odoi for their advice, critique, encouragement, and direction that made this work to be completed. I am also thankful to all my lecturers who provided academic tutelage for my formative year and during my research work.

My deepest thanks go to the International Atomic Energy Agency (IAEA) for awarding me a scholarship and also for my employers National Institute for Scientific and Industrial Research (NISIR) for granting me a study leave to pursue my studies. I would like to acknowledge Argonne National Laboratory (ANL) the developers of the codes that were used for this work.

I would like to thank my family for their prayers and encouragement during my studies.

Last but not the least, I would like to thank all my friend for the knowledge and ideas we shared during the course and research work.

TABLE OF CONTENTS

LIST OF TABLES

LIST OF FIGURES

ABBREVIATIONS

ANL	Argonne National Laboratory
ANS	American Nuclear Society
CIAE	China Institute of Atomic Energy
DNBR	Departure from Nucleate Boiling Ratio
FIR	Flow Instability Power Ratio
FTC	Fuel Temperature Reactivity Coefficient
GAEC	Ghana Atomic Energy Commission
GHARR-1	Ghana Research Reactor-1
HEU	Highly Enriched Uranium
IAEA	International Atomic Energy Commission
LPPR	Low Power Pool Reactor
MCNP	Monte Carlo Neutron Particle
MNSR	Miniature Neutron Source Reactor
MTC	Moderator Temperature Coefficient
NNRI	National Nuclear Research Institute
PARET/ANL	PLate TEMPerature Analysis code
REBUS/ANL	REactor BUrnup System code
RTC	Reactivity Temperature Coefficient
SAR	Safety Analysis Report
STAR-CCM+	STAR Computational Continuum Mechanics code

LIST OF SYMBOLS

k_{eff}	Neutron Multiplication factor
N_o	Neutrons in the preceding generation
ρ	Reactivity
$\dot{\rho}$	Rate of change of reactivity
λ_{eff}	Effective delayed neutron precursor decay constant
β_{eff}	Effective delayed neutron fraction
Λ	Neutron generation time
l_p	Neutron life time
ρ_{crw}	Reactivity for control rod withdrawn
ρ_{in}	Reactivity due to control rod fully inserted in the core
ρ_{out}	Reactivity due to control rod fully withdrawn
ρ_{sdm}	Reactivity shutdown margin
V	Average neutron velocity
ν	Average number of neutrons produced
Σ_f	Fission macroscopic cross section
Σ_a	Macroscopic absorption cross section,
B	Geometrical buckling
D	Diffusion coefficient
ΔT	Temperature difference
H	Height of core inlet orifice
T	Temperature
P	Power of the reactor

ϕ	Average neutron flux
V_f	Volume of the core
h	Core height
r	Core radius
q''	Heat flux $(\frac{W}{m^2})$
q'''	Volumetric heat source
u	Coolant velocity
$\dot{m}$	Mass flow rate
Ψ	Pressure
G	Fission energy deposited in the fuel
E	Energy
k	Thermal conductivity$\left(\frac{W}{m-K}\right)$
c_p	Specific heat capacity
t	Time
h_{fg}	Transition heat
h_g	Vapor phase heat
h_f	Liquid phase heat
T_{sat}	Saturation temperature
N	Number of Neutron history
I_g	Number of cycles to skip in MCNP simulation
I_t	Total number of MCNP simulation cycles
I_A	Number of MCNP simulation active cycles
K_p	Multiplication factor for prompt neutrons
b	Barn. Unit equivalent to $10^{-24} cm$.

ABSTRACT

Evaluation of safety parameters of GHARR-1 after nineteen years of operation were performed and are presented herein. This work serves as an input into periodic evaluations of safety parameters. Due to fuel depletion, the excess reactivity for GHARR-1 drops to the allowed lower limit of 2.3 mk from 4 mk in about 2 years. Beryllium is added to the top shim tray of the core to compensate for reactivity loss. The addition of beryllium to the top of the core requires evaluations of safety parameters. The objective for this work was to evaluate the safety parameters of GHARR-1after 19 years of operation and compare them with those provided in the SAR and other literature. Four codes namely; REBUS/ANL, MCNP, PARET/ANL and PLTEMP/ANL were used in this work. The REBUS/ANL code was used to generate an inventory of isotopes in the fuel after 19 years of operation. The masses for the isotopes were used to update the material card in the MCNP model for GHARR-1 and 9 mm of beryllium was also added to the top shim tray in the model. The MCNP code was used to predict neutronics and kinetic parameters of GHARR-1. The neutron generation time, delayed neutron fraction, axial power peaking factors, fuel temperature reactivity coefficient, moderator temperature coefficient and the moderator void coefficient were used in the PARET/ANL code to predict the transient and steady state parameters of the reactor. The existing PLTEMP/ANL input deck was updated with the axial and radial power peaking factors obtained from the MCNP simulations. The code was used to predict the steady state parameters; DNBR, ONBR, FIR, saturation and ONB temperatures respectively. The delayed neutron fraction, neutron generation time, moderator reactivity coefficient were

predicted as; $8.17507\times10^{-3}\ \Delta k/k$, 8.147×10^{-5} s ,-0.1218 mk which compared with those provided in the SAR as $8.08\times10^{-3}\ \Delta k/k$, 8.12×10^{-5} s ,-0.13 mk. The maximum power peaking factor was predicted as 1.3522 compared to 1.3525 for the clean core and it was with the expected range of 1.3 to 1.5 for light water reactors. The reactor power for reactivity insertion of 2.1 mk was predicted as 39.3 kW compared to 36.1 from experimental work. The DNBR, ONBR and FIR for 30 kW were predicted as; 19.12, 1.25, and 4.37, respectively. The results obtained indicate that the reactor's neutronic and thermal hydraulic characteristics meet requirements set out in the Safety Analysis Report.

CHAPTER ONE

INTRODUCTION

1.1 BACKGROUND

Research reactors play critical roles in the advancement of nuclear science and technology worldwide. As of 2013 there were 731 research reactors worldwide including those under construction and planning stages. Out of the 731 research reactors, 20 were in temporal shut down condition, 4 were under construction, 8 were being planned, 148 had been shut down, and 306 had been decommissioned [1]. Of these research reactors, only 10 were in Africa which accounted for 1.36 percent. Despite this small number, Africa's research reactors are a vital component that have significantly contributed to scientific progress and the evolving role nuclear science and technology plays in society [2].

A nuclear reactor is a complex structure with a lot of interrelated systems and components that complement in initiating, sustaining and control of a fission chain reaction. These systems and components are governed by various neutronic, thermal-hydraulic and mechanical properties. These properties play important roles in the safe operation of reactors and as such, various operational parameters are established to ensure the existence of safety margins between normal operations and safe limits. The existence of these operational parameters and safety margins ensure safe operation of the reactor with enhanced safety of the operators and the general public at large.

The potential for hazard to the public that is posed by research reactors is minimal compared to that posed by nuclear power reactors. However, research reactors cause

potential hazard to operators. The potential hazard posed by research reactors vary depending on the type and their associated uses. As such, in the quest to achieve adequate safety, application of a graded approach to safety analysis should be commensurate with the potential hazard [3].

As a reactor operates, there is an increase in fuel burnup which leads to the neutron spectrum becoming softer due to buildup of fission products. Some of the fission products produced have a high affinity for neutrons and as such they adversely affect the neutron population and proportionally, reactor power. Such fission products are called neutron poisons.

The buildup of fission products in the fuel make reactivity coefficients more negative [4]. Besides these changes in the fuel composition and reactivity coefficients that occur over a long period of time, there are also fluctuations that occur during normal operations of a reactor. A typical example of such fluctuations is observed in reactor power. The fluctuations in reactor power during normal operations has an effect on the temperature profile along a coolant channel [5]. This in turn causes variations in the departure from nucleate boiling ratio (DNBR) which may consequently reduce the safety margins [6].

Any activity that may influence neutronic, thermal-hydraulic and mechanical properties of the reactor should be supported by periodic safety evaluations.

The behaviour of neutrons in the reactor is studied under neutronics. This is an important field whose outputs are critical for safety analysis for both research and design considerations. The safety analysis is supported by reactivity and dynamic response characteristics. Neutronic analyses in general cover; excess reactivity, shutdown margin, control rod worth, rod worth profile, power distribution, power peaking factors, kinetic parameters (e.g prompt neutron life time, effective delayed neutron fraction) and reactivity feedback coefficients (e.g. temperature reactivity coefficients) [7]. These neutronic parameters have an effect on thermal hydraulic parameters.

Thermal-hydraulics deals with the feedback effects such as heat transport, fluid flow and mechanical changes. Steady-state thermal hydraulics cover safety margin calculations, for example, margin to the onset of nucleate boiling (ONBR), coolant saturation temperature, onset of flow instability power ration (FIR), departure from nucleate boiling ratio (DNBR) and critical heat flux temperature [7].

The limit set on the operational power of a reactor core is largely due to thermal hydraulics and not nuclear considerations. The allowable core power is restricted by the efficiency with which heat is removed from the fuel into the coolant. Failure to effectively remove heat from the fuel would lead to degradation of the fuel and the fuel cladding [8].

The interaction between neutronic and thermal-hydraulic properties of a nuclear reactor core is an essential and fundamental facet of nuclear core performance. The various negative reactivity coefficients contribute to a nuclear reactor's inherent operational stability and safety. [9]

1.2 STATEMENT OF THE PROBLEM

The GHARR-1 research reactor has been in operation for nineteen (19) years. A 9 mm shim of beryllium has been added to the top shim to compensate for the loss in excess reactivity due to buildup of poisons within the fuel. Despite the addition of beryllium and restoration of the excess reactivity to about 4.0 mk, some of the changes in parameters that occur relative to fuel burnup are independent of the effect of beryllium addition. For example, the buildup of fission products cannot be reversed by the addition of beryllium. As such, it was imperative to study the effects that these non-reversible changes have on neutronics and thermal hydraulics of the irradiated core of GHARR-1.

Eventhough GHARR-1 has been in operation for 19 years with the addition of 9 beryllium to the top shim tray, most modelling and simulation works that have been carried out have not taken into account updating the composition of the fuel after 19 years of operation. As such, there has been a data deficit on coupled neutronics and thermal hydraulics of the irradiated core of GHARR-1.

1.3 RELEVANCE AND JUSTIFICATION

This work couples neutronics and thermal-hydraulics and provides data on the current status of GHARR-1's safety parameters relative to nineteen (19) years of operation and addition of beryllium to the top shim tray. Data generated from this work will be used for academic purposes and as a basis for comparison with similar works to be carried out in future. More up to date data on GHARR-1 generated from this work will be used to

supplement that which already exists. Data generated could also be used as an input into the next Safety Analysis Report (SAR) of GHARR-1.

The principal beneficiaries of this work are reactor operators and users of the facility, as it will provide them with data on the current status of the safety parameters in relation to set safety margins.

1.4 RESEARCH OBJECTIVES

1.4.1 Main Objective

1.4.1.1 To evaluate the safety parameters of GHARR-1 after nineteen(19) years of operation

1.4.2 Specific Objectives

1.4.2.1 To predict neutronic parameters of GHARR-1.

1.4.2.2 To employ neutronic parameters to predict thermal-hydraulic parameters.

1.4.2.3 To compare the safety parameters with those provided by the manufacturer during initial startup.

1.5 SCOPE AND DEFINITION

This work covers neutronics and thermal hydraulics safety parameters of GHARR-1 and their interplay. Under neutronics, the following safety parameters have been investigated; shutdown margin, control rod worth, excess reactivity, fuel temperature reactivity

coefficient, void reactivity coefficient, moderator temperature reactivity coefficient, moderator reactivity coefficient, axial and radial power peaking factors, delayed neutron fraction, and prompt neutron generation time. Under thermal-hydraulics, fuel centerline temperature, cladding temperature, coolant temperature, DNBR, ONB, FIR, and coolant saturation temperature have been investigate.

1.6 LIMITATIONS

This work does not cover mechanical and electronic safety assessment as it is a different field from that discussed in this thesis.

1.7 THESIS OUTLINE

Chapter Two presents the literature survey on neutronics and thermal-hydraulics. It outlines works that have been carried out on parameters that are relevant to this work. Under this chapter, parameters that were evaluated are defined and in some cases derived mathematically. Neutronics covers the multiplication factor, excess reactivity, and shutdown margin whereas the kinetic parameters cover, delayed neutron fraction and neutron generation time. Under thermal-hydraulics, heat generation, heat flow, temperature dependence on power, steady state and transients are covered. Different methods of determining safety parameters are also presented.

Chapter Three discusses the method of solution for the various parameters that are analysed in this work. The applications of REBUS/ANL, MCNP5/ANL, PARET/ANL and PLTEMP/ANL codes in determining and predicting parameters described in chapter two is outlined. The link between the output of one code and how they are applied in another code is described.

Chapter Four is devoted to presentation of results, observations, analysis and discussions for 61 simulations that were done for this work.

Finally, chapter five gives a summary of the work done, draws conclusions and recommends possible future work.

CHAPTER TWO

LITERATURE REVIEW

There exist feedback effects amongst the nuclear, fluid, thermal, chemical, and structural behaviour of a nuclear reactor. The performance of a reactor core is fundamentally attributed to the interplay between thermal-hydraulics and neutronics. This interplay between thermal-hydraulics and neutronics is called reactivity feedback or thermal feedback.

There has been an increase in research activities that seek to couple neutronics and thermal hydraulics. This has led to development of codes that couple the versatile Monte Carlo Neutron Particle transport code (MCNP) and other thermal hydraulics analysis codes. All these efforts are being made to enhance the understanding of the interplay between the two fields. These studies, inter alia, aim at improving the safety operations of nuclear reactors and also to ensure that optimal operational safety margins are established.

The IAEA-TECDOC-1332[10] has defined safety margin of operating reactors as the difference or ratio in physical units between the limiting value of a parameter, of which operating beyond the limiting value leads to failure of a system or component, and the real operational value of that parameter in the reactor. The presence of these operational margins ascertains the reactor would often operate safely in all modes.

Cardoni J. N and Rizwan-uddin[11] carried out nuclear reactor multi-physics simulations with coupled MCNP5 and STAR-CCM+ codes. The study outlined that there exists

feedback effects amongst the nuclear, fluid, thermal, chemical, and structural behaviour of a nuclear reactor. The interplay between the neutronic and thermal-hydraulic properties of a nuclear reactor core, called thermal or reactivity feedback, is a fundamental aspect of nuclear core performance. The negative temperature reactivity coefficient contributes to a nuclear reactor's inherent operational stability and safety. In pressurized water reactors, thermal feedback and temperature coefficients of reactivity are primarily from microscopic cross section's temperature dependence and from the change in moderator density with temperature. Microscopic cross section's temperature dependence is a result of the Doppler effect. The Doppler effect is a change in cross section due to temperature changes altering the thermal motion of a nuclei [12].

In general, an increase in temperature lowers and widens resonance peaks to preserve the total area under the resonance. Although numerically smaller than the reactivity coefficient due to moderator temperature change, the reactivity feedback effect from the Doppler effect is almost instantaneous, making it a vital characteristic in nuclear reactor performance. In a low enriched PWR, the Doppler effect decreases reactivity due to parasitic absorption in epithermal U-238 resonances.

Ampomah-Amoako et *al.* [13], studied the transient behaviour of GHARR-1 using PARET/ANL thermal hydraulic code. It was established from his work that the reactor was safe to operate with reactivity insertion range of 2.1mk to 4 mk. However, the code was not able to simulate reactivity insertions above 5 mk. This was attributed to different fluid flow regime of the reactor that were considered. It was observed that for 2.1mk

reactivity insertion, the peak power was 54.8 kW as compared to 36 kW and 36.8 kW from experiments that were carried out by Akaho et *al*. [14].

The model that was used in the study was a modification of the PARET/ANL model that had been used by Olson and Jonah [15] in which changes were made to the heat source for moderator, critical mass, single phase correlation flag, total cross-sectional area of all flow channels in the core and the reactivity insertions. The power peaking factor for the 21 axial sections were acquired from the work that was carried out by Anim-Sampong [16] in which the GHARR-1 MCNP model was simulated with particle history of 120,000 with 400 active cycles each. Transients were studied for 3000 s with reactivity insertion for 2.1 mk, 4.0 mk and 6.71 mk.

Adoo [17] carried out similar studies to determine the thermal hydraulic parameters of GHARR-1. The work applied the PARET/ANL thermal hydraulic code for which reactivity insertions ranged from 2.0 mk to 5.5 mk. The study showed that the peak clad and coolant temperatures ranged from 59.18 °C to 112.36 °C and 42.95 °C to 79.42 °C. The values obtained from the study were in good agreement with the MNSR thermal hydraulic design benchmarks for which boiling does not occur in the reactor core. The study showed that the negative reactivity feedback of the moderator for GHARR-1 is a desirable inherent safety feature which limits power excursion and the corresponding escalation of the clad temperature. The excess reactivity was predicted to be less than $\beta_{eff}/2$ which is an important value that prevents the possibility of prompt criticality being attained.

In 2012, Boafo [18] assessed the effects of fuel burn up on control rod worth for GHARR-1 using the MCNP code. The study highlighted that control rod worth is affected by factors such as fuel burn up, Xenon concentration, Samarium concentration and control rod position in the core. The fuel burn up was calculated using a deterministic code BURNPRO which uses three energy groups; fast, resonance and thermal respectively. Modifications to the MCNP input deck developed by Anim-Sampong [16] were made with additions of isotopes such as U-236, Pu-239, Pu-240 and Pu-241 to reflect the changes in the fuel composition. The depletion in concentrations of U-235 and U-238 were also changed accordingly. In order to analyze the effect of burnup on control rod worth, the irradiated and fresh MCNP models of GHARR-1 were used for the simulations. The study indicated that with 1.16% fuel burnup, there was a corresponding increase in control rod worth from 6.4mk to 7.4mk and a reduction in the flux level in the irradiation sites.

Ahmed [19] studied the behaviour of reactor power and flux due to changes in the core coolant temperature for the Nigerian Research Reactor-1 (NIRR-1) a Miniature Neutron Source Reactor (MNSR) which has similar features as GHARR-1. The study indicated that due to safety requirements, in order to study reactor power and flux behaviour relative to changes in core-coolant temperature, it is imperative to carry out several measurements [20, 21]. The study stressed out two safety factors that were taken into account in the design and construction of the MNSR and also during the Zero power experiments. These factors were; the hydrogen to uranium ratio which was set to be 197

which is similar to that of GHARR-1 and the core-height to diameter ratio which was set at 1.0. The hydrogen to uranium ratio was set so as to increase the degree of under moderation of the core. This has an effect of making the negative temperature coefficient more negative and at the same time enhancing the temperature feedback effect. The optimization to 1.0 of the core height to diameter was done to enhance two factors; increase the worth of the top beryllium reflector thus extend the life of the core and also to support coolant flow and mixing thus shortening the time of temperature feedback. Besides the afore mentioned factors, the design requires that the inlet and outlet orifices be maintained at 6 mm and 7 mm respectively so as to yield the desired rise in temperature of the coolant.

The results indicated that during reactor operation, the position of the control rod rose with time as a way of compensating the negative temperature coefficient. The rise in control rod position also keeps the reactor power at a preset level. This mechanism satisfies one of the safety features of the reactor which prevents power excursion and occurrence of boiling.

The results obtained from the work indicated that thermal hydraulics data and neutronics parameters could be used to predict the reactor's operating power. On the other hand, the data generated from the work indicated that the operating power level of the reactor can be estimated from preset thermal neutron flux values.

Alhassan [22] studied the reactivity temperature coefficient for light water moderated MNSR with HEU-UAl_4 and LEU-UO_2 lattices. The study stressed three critical safety mechanisms that affect reactivity in the reactor. These were spelt out as; fuel, moderator expansion, and void production feedbacks. These inherent safety features are provided in

MNSR designs through the high negative reactor temperature coefficient (RTC) which affects the three safety mechanisms outlined above.

The MCNP code was used for the analysis and it was based on the Pin Cell model in which the fuel materials in the reactor core is lumped together and treated as one fuel rod surrounded by the lumped moderator material.

Based on the Pin Cell model, the moderator temperature coefficient (MTC) was predicted by analyzing its effect on the six factor formula. The MTC has a strong dependence on the thermal utilization factor.

The fuel temperature coefficient (FTC) was studied by obtaining a product of the effective multiplication factor and the six factor formula and thus analyzing the change of the fuel temperature in relation to each of the factors. The FTC was predicted by studying the resonance escape probability as it was established that the temperature effect on fuel is largely due to the Doppler broadening of resonances. The FTC was calculated by varying the fuel temperature and computing the corresponding cross section.

Daniel [23], carried out safety analysis of an accident reactivity excursion for the University of Florida Training Reactor. The study indicated that moderator coefficient of reactivity is a function of varying moderator voiding (density) and the absorption of neutrons with changes in moderator temperature. The MCNP analysis of the variation in water's cross section relative to increased temperature was inconclusive. This is attributed to the observed change in reactivity that did not exceed the reported three standard deviation range.

The Moderator coefficient of reactivity was predicted by perturbing the coolant density (coolant void) and fuel temperature in the MCNP model. The multiplication factors (keff) obtained were analysed using the respective reactivity equations. The coolant voiding and temperature ranges that were considered included normal operations and accident scenarios.

The fuel temperature coefficients obtained indicated that there is non-linearity in the reactivity feedback to fuel temperature variation over a wide range. This facet is important to consider when selecting coefficients to employ when coupling thermal-hydraulics/neutronics analysis for transients where the expected range of fuel and coolant conditions have to be taken into account.

Unlike the fuel temperature coefficient, the moderator void coefficient was observed to be linear as it is independent of the effect temperature has on fuel cross section. Currently there is no direct method for voiding water in the MCNP model. As such the moderator void coefficient was analysed by changing the density of water in the MCNP model. This is an accurate way of voiding water in the MCNP model. The study indicated that, the elevation of the reactor relative to the sea level and the atmospheric pressure should be taken into account when making changes to the density. The MCNP PERT card was used to vary the density.

Bretscher et *al.* [24] studied the neutronics and carried out transient analyses of Poland's Maria Research Reactor. The transient analyses, control rod reactivity worth, reactivity

feedback coefficients, kinetic parameters, and power distributions were computed for the 16 fuel assemblies of the MARIA reactor. The prompt neutron generation time was predicted using the 1/v insertion method for fresh and burned HEU fuel and for fresh LEU. The results demonstrated that as the spectrum hardens, the prompt neutron generation time decreases. This is an expected trend when HEU fuel is replaced with LEU fuel. The delayed neutron fraction was predicted using a perturbation code and ENDF/B-VI delayed neutron data.

The temperature reactivity feedback coefficients for the temperature range 27 °C to 277 °C was determined using 2^{nd} order (linear) fits whereas, the void reactivity feedback coefficients were determined using the 4^{th} order polynomial fit. All reactivity coefficients for the MARIA reactor were determined to be negative except for the beryllium temperature feedback coefficient.

The 1/v insertion method was employed in determining prompt neutron lifetimes and prompt neutron generation times for fresh and irradiated core with HEU and LEU fuel lattices.

The results demonstrated the anticipated behaviour that as the neutron spectrum hardens when HEU fuel is replaced with LEU fuel, the prompt neutron lifetime decreases.

The void and Temperature reactivity coefficients were obtained for the two fuel lattices. The above mentioned reactivity coefficients and their uncertainties were evaluated by the least square method in which a set of Eigen values were fitting to a polynomial. Taking

into account statistical considerations, it was concluded that the temperature reactivity coefficients are best determined by 2nd order fit in the temperature range 300 K-550 K. The void coefficient was, however, determined by a 4th order polynomial fit.

2.2 DESCRIPTION OF GHARR-1 MNSR

2.1.1 General Description of the Facility

The Ghana Research Reactor-1 (GHARR-1) is a low power research reactor (LPRR) with 30 kW nominal power. It is a small, safe nuclear facility, which employs highly enriched uranium (HEU) as fuel, light water as moderator, coolant and shield, and beryllium as a reflector. The reactor is cooled by natural convection.

The reactor is a commercial Miniature Neutron Source Reactor (MNSR) manufactured and constructed by the China Institute of Atomic Energy (CIAE), Beijing, China. It is designed to be used for academic purposes in universities, generation of radio isotopes in hospitals, neutron activation analysis, education, and human resource development in research institutes.

The reactor is located at the National Nuclear Research Institute (NNRI) of the Ghana Atomic Energy Commission (GAEC). The reactor has a simple structure with a small volume. It is convenient and reliable in operation and its construction and operation costs are low [25].

2.1.2 Core Description of GHARR-1

The GHARR-1 consists of 344 fuel pins, 4 tie rods and 6 dummy pins concentrically arranged in 10 rings. The fuel assembly, rests on a 50 mm block of beryllium reflector, surrounded by a 100 mm thick annular beryllium reflector, and a top-shim tray which allows addition of beryllium reflector. The core has a central guide tube through which a Cadmium control rod cladded in stainless steel moves to cover the core active length of 230 mm. The control rod serves as a regulation for power, compensation of reactivity, and for reactor shut down during normal and abnormal operations [26]. Figure. 2.1 shows a schematic diagram of the vertical cross-section of the reactor of GHARR-1 with 9 mm thickness of beryllium added to the top-shim tray.

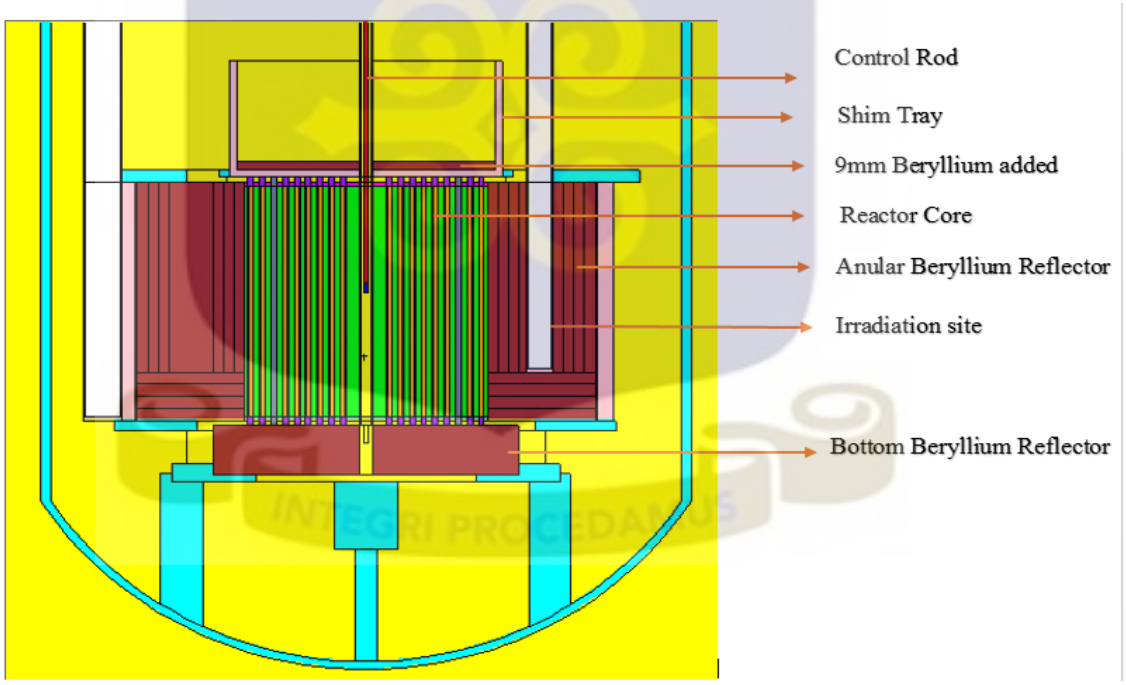

Figure 2.0. A schematic diagram of the vertical cross-section of GHARR-1

Table 2.1Specifications of GHARR-1[25]

No.	PARAMETER	VALUES
1	Reactor type	Tank in pool
2	Rated thermal power	30 kW
3	Fuel Type	Rod
4	Fuel rod positions	150
5	Fuel element loading	344
6	No. of dummy elements	6
7	Fuel lattice pitch	10.95 mm
8	Fuel composition	U-Al4 dispersed in Al
9	Fuel density	3.456 g/cm^3
10	Dummy element material	Al
11	Cladding material	Al alloy (LT-21)
12	Uranium Wt. (%)	27.5
13	U-235 Enrichment (%)	90.2
14	Burn-up (%)	~1
15	Loading of U-235 in the core (g)	998.12
16	Temperature coefficient	~-0.10 mk/°C (Average)
17	Active fuel length	230 mm
18	Coolant/Moderator	Deionised H_2O
19	Coolant/Moderator Density	995.1 kg/m^3
20	Coolant Flow Rate	400 L/hr
21	Coolant inlet Temperature	30 °C
22	Coolant inlet pressure	101.3 kPa ~1 bar
23	Coolant mode	Natural convection

24	Reflector	Beryllium
25	Control rod absorber	Cadmium
26	Control rod cladding	Stainless steel
27	Control rod length	230 mm
28	Number of control elements	1
29	Core shape	cylindrical
30	Core diameter	230 mm
31	Core height	230 mm
32	Excess reactivity-cold clean	4 mk
33	Total number of irradiation sites	10
34	Inner irradiation sites	5 (3 large, 2 small)
35	Maximum thermal Neutron flux	1.0×10^{12} n/cm^{2}s (at rated power)
36	Outer irradiation sites	5 (3 large, 2 small)
37	Maximum thermal Neutron Flux	5.0×10^{11} .n/cm^{2}s (at half rated power)
38	Effective delayed neutron fraction	8.08×10^{-3}
39	Prompt neutron lifetime	8.12×10^{-5} s

2.1.3 Reactivity Control Criteria

The reactor is controlled either through the main control console or via a micro-computerised control system. The design of the control system follows the relevant guidelines, standards as well as the general requirements of control functions. The control system of GHARR-1 is in accordance with the Chinese national standards and guidelines [25] and approved by the Ghana Radiation Protection Authority and the International Atomic Energy Agency (IAEA).

The control range of the automatic control system is designed to cover $10^8 - 10^{12}\ n/m^2.s$ The control accuracy is ±1% of the maximum value of the range. The design control rod worth of the reactor is 6.8 mk with a shutdown margin is 3.0 mk for maintaining the reactor in safe shutdown condition. The total cold excess reactivity to be compensated by the control rod is approximately 4.0 mk. According to requirements of ANSI/ANS-15-1978 "Criteria for the reactor safety systems of research reactors" scram systems are to be provided for the reactor power regulations and thermo-hydraulic system. The settings for the reactor scram are such that the reactor power should not exceed 120 % of the nominal power of 30 kW and the temperature difference between the core outlet and inlet should not exceed 120 % of its nominal limit (30°C). The reactor can additionally be shut down by pumping cadmium rabbits with negative reactivity into the inner irradiation sites through the rabbit system [27].

2.1.4 Operational mode of GHARR-1

The Ghana Research Reactor GHARR-1 became critical in 1995 and has a fuel burn up of 1%. It was designed with a lifetime core of 10 years if it is operated at its maximum power of 30kW for 2.5 hours a day, five days a week . The reactor is designed to have inherent safety features which limit peak power levels in an event of reactivity inserted accidentally. These safety features are; the high negative moderator temperature coefficient of reactivity (approximately -0.l mk/°Cat a temperature range of 20 to 45 °C), low critical mass, and under moderation. With these safety features, safety of the reactor is achievable under all conceivable accident conditions [25].

The reactor core has a very small margin (1.7 mk) of excess reactivity for operation which is between 4.0 mk and 2.3 mk. Due to xenon buildup, the reactor cannot be operated continuously. It is designed to operate for a short time; not more than 4 hours at 15 kW and not more than ~ 2 hours at 30 kW.

The GHARR-1 is operated on a 15 kW (for 4 hours per day, 4 days per week, and 52 weeks per year) scheme. Under this scheme, the excess reactivity drops to about 2.3 mk lower limit in about 1.96 years. Beryllium shim plates are then added to the top shim tray to compensate for loss in excess reactivity. This restores the core excess reactivity to the design value of 4.0 mk and begins the next reactor operational cycle. The MNSR fuel cycle is thus be defined on the basis of the shim cycle length; as the time taken for the core design excess reactivity to drop to the set lower limit necessitating the addition of a layer of beryllium [33].

Beryllium is used as a reflector because of its high neutron scattering cross section. The use of beryllium as a reflector reduces neutron leakage out of the core and thus helps to conserves the neutron economy.

2.2 NEUTRONICS

Nuclear reactor performance is fundamentally governed by the behaviour of neutrons in the core. The interactions of neutrons with core materials bring about a number of effects such as; nuclear fission, heat generation, and induced radioactivity in reactor materials. These effects, lead to various reactor aspects such as reactivity control, reactor kinetics, xenon stability, fuel depletion, and isotope production which play an integral part in the quest to understanding reactor performance and safety. The distribution of neutrons in the core plays a central role in establishing a power distribution and heat transfer profile. There are strong feedback effects between nuclear physics and the other physical processes in the reactor, particularly thermal-hydraulics [31].

2.2.1 Multiplication Factor

The operation of a Nuclear reactor requires a sustainable chain reaction. This is achieved by the ability of neutrons, emitted in fission reaction, to cause further fissions in other fissile or fissionable nuclei. The fission chain reaction is quantitatively expressed in terms of the multiplication factor (k_{eff}). The neutron multiplication factor is defined as a ratio between the number of neutrons in the current generation to the number of neutrons in the preceding generation. It is mathematically expressed as;

$$k_{eff} = \frac{\text{Number of neutrons in one generation}}{\text{Number of neutrons in preceding generation}} \qquad 2.0$$

When k_{eff} = 1 the reactor is designated as being critical.

$k_{eff} > 1$ the reactor is defined to super critical.

$k_{eff} < 1$ the reactor is defined as being subcritical.

2.2.2 Excess Reactivity

A measure of the departure of the reactor from criticality is referred to as reactivity. Reactivity is defined as the fractional change in neutron population per generation.

If there are N_o neutrons in the preceding generation, then taking into consideration the multiplication factor k_{eff}, there will be $N_o k_{eff}$ neutrons in the current generation. Therefore, reactivity ρ will be expressed as;

$$\rho = \frac{N_o k_{eff} - N_o}{N_o k_{eff}} \qquad 2.1$$

Factoring out N_o and solving the Equation 2.1 leads to Equation 2.2.

$$\rho = \frac{k_{eff} - 1}{k_{eff}} \qquad 2.2$$

As a reactor operates, there is a gradual decrease in the amount of fuel loaded in the core. If the reactor is loaded with the exact amount of fuel required for it to be criticality, the reactor will, within a short time, fail to sustain criticality and it would eventually shutdown as the number of neutrons would continue decreasing as the fuel depletes. To avert this problem, fuel in excess of that required to make a reactor critical is added to the reactor core when the reactor is built. The positive reactivity due to the excess fuel is referred to as excess reactivity [34]. This excess reactivity is balanced by the addition of materials in the core that have high neutron absorption cross section (poisons) that absorb the excess neutrons.

The GHARR-1, uses a central control rod for controlling the excess reactivity. The excess reactivity is restricted to $\frac{1}{2}B_{eff}$ to ensure prompt criticality does not occur. This can be deduced from Equation 2.3. If $B_{eff} = \rho$ then the second term in Equation 2.3 would vanish and only the prompt term would remain and the reactor would turn prompt critical which is not desired as this will favor power excursion within seconds.

$$\tau = \frac{\Lambda}{\ell} + \frac{\bar{\beta}_{eff} - \rho}{\lambda_{eff}\rho + \dot{\rho}} \quad 2.3$$

where Λ is the neutron generation time,

ρ is reactivity

$\bar{\beta}_{eff}$ is effective delayed neutron fraction

λ_{eff} is effective delayed neutron precursor decay constant

$\dot{\rho}$ is rate of change of reactivity

$\frac{\Lambda}{\ell}$ is the prompt term

$\frac{\bar{\beta}_{eff} - \rho}{\lambda_{eff}\rho + \dot{\rho}}$ is the delayed term

2.1.1 Control Rod Worth

Control rod worth is the efficiency of a control rod to absorb the excess reactivity. It is an important parameter in the design and analysis of nuclear reactor core [18]. For reactors like GHARR-1, with a single control rod, Control rod worth is determined as the difference between the reactivity inserted when the control rod is fully withdrawn and that inserted when fully inserted. It is mathematically expressed as shown in Equations 2.4 and 2.6.

$$\rho_{crw} = \rho_{in} - \rho_{out} \qquad 2.4$$

where ρ_{crw} is the control rod worth

ρ_{in} is reactivity when the control rod is fully inserted

ρ_{out} is reactivity inserted when the control rod is fully with drawn

Expressing Equation 2.4 in terms of the multiplication factor gives

$$\rho_{crw} = \frac{k_{eff_{out}} - 1}{k_{eff_{out}}} - \frac{k_{eff_{in}} - 1}{k_{eff_{in}}} \qquad 2.5$$

which reduces to Equation 2.6

$$\rho_{crw} = \frac{k_{eff_{out}} - k_{eff_{in}}}{k_{eff_{out}} k_{eff_{in}}} \quad 2.6$$

2.3.3 Shutdown Margin

Shutdown margin is defined as the negative reactivity provided in addition to that needed to keep the reactor in a subcritical condition without a time limit. It is given by a mathematical relation represented by Equation 2.7 which expresses the difference between the control rod worth and the excess reactivity.

$$\rho_{sdm} = \rho_{crw} - \rho_{ex} \quad 2.7$$

Substituting Equations 2.2 and 2.6 into Equation 2.7 gives us

$$\rho_{sdm} = \frac{k_{eff_{out}} - k_{eff_{in}}}{k_{eff_{out}} k_{eff_{in}}} - \frac{k_{eff_{out}} - 1}{k_{eff_{out}}} \quad 2.8$$

Equation 2.8 reduces to Equation 2.9

$$\rho_{sdm} = \frac{k_{eff_{out}} - k_{eff_{in}} - k_{eff_{out}} k_{eff_{in}} + k_{eff_{in}}}{k_{out} k_{in}} \quad 2.9$$

thus Equation 2.10 give the expression of shutdown margin as a function of k_{eff}

$$\rho_{sdm} = \frac{1 - k_{eff_{in}}}{k_{eff_{in}}} \quad 2.10$$

2.3 KINETIC PARAMETERS

2.3.1 Delayed Neutron Fraction

Delayed neutrons have a great impact on reactor dynamics and this can be understood through their influence on the rate at which reactor power changes. They play a dominant role in chain reaction control. Despite having this crucial property, they only constitute a very small fraction of the total number of neutrons produced as a result of fission.

Delayed neutrons have an average lifetime of 12.2s whereas prompt neutrons have an average life time of 10^{-4} s. If a reactor operated only with prompt neutrons, it would be prompt critical and impossible to operate due to rapid changes in reactor power. As a reactor operates, delayed neutrons play an important role during operation of a reactor during power transients. As such, accurate prediction of the delayed neutron fraction value is critical in nuclear physics. An accurate prediction of B_{eff} is essential for converting reactivity expressed in dollars, to an absolute reactivity and absolute k_{eff} .

2.3.2 Neutron Generation Time

The prompt neutron generation time (Λ) is the average time from birth of a neutron to a point it reproduces itself by fission. The prompt neutron generation time can also be defined as the inverse of the neutron production rate as expressed by Equation 2.11. This is applicable when considering a one-group diffusion-theory approximation.

$$\Lambda = \frac{1}{V\nu\Sigma_f} \qquad 2.11$$

Where Λ in the average neutron velocity, ν is the average number of neutrons produced per fission and Σ_f in the fission macroscopic cross section.

There is however a difference between neutron generation time and neutron life time. Neutron life time is defined as the time length between the birth of a neutron and its absorption. In this work the neutron generation time is used to determine the neutron generation time. A detailed use of this parameter is explained in Chapter 3. Neutron lifetime is expressed as the inverse of neutron destruction rate described by equation 2.12.

$$\ell = \frac{1}{V\left(\Sigma_a + DB^2\right)} \qquad 2.12$$

Where Σ_a is the macroscopic absorption cross section, B is the geometrical buckling, D is the diffusion coefficient and k_{eff} is the steady-state effective multiplication factor.

2.4 CONTROL ROD CURVE

Figure 2.3 shows a curve of the integral control rod worth against core depth. The amount of reactivity inserted relative to control rod withdrawal is highest around the center of the core. It can be seen from the curve that around the center of the core, a small change in control rod position causes a large reactivity change. This is as a result of the high neutron density in the center of the core.

A plot of the integral control rod worth slop is shown in Figure 2.2. This plot is the rate of change of control rod worth with change in position. Such a plot is referred to as the differential control rod worth. At the bottom of the core there are few neutrons so rod

movement has little effect; therefore the change in rod worth over distance is nearly constant. As the rod approaches the center of the core its effect becomes greater, and the change in rod worth per distance becomes significant. At the center of the core, the differential rod worth is greatest and varies little with rod motion. From the center of the core to the top, the rod worth per distance is the opposite of the rod worth per distance from the center to the bottom [35].

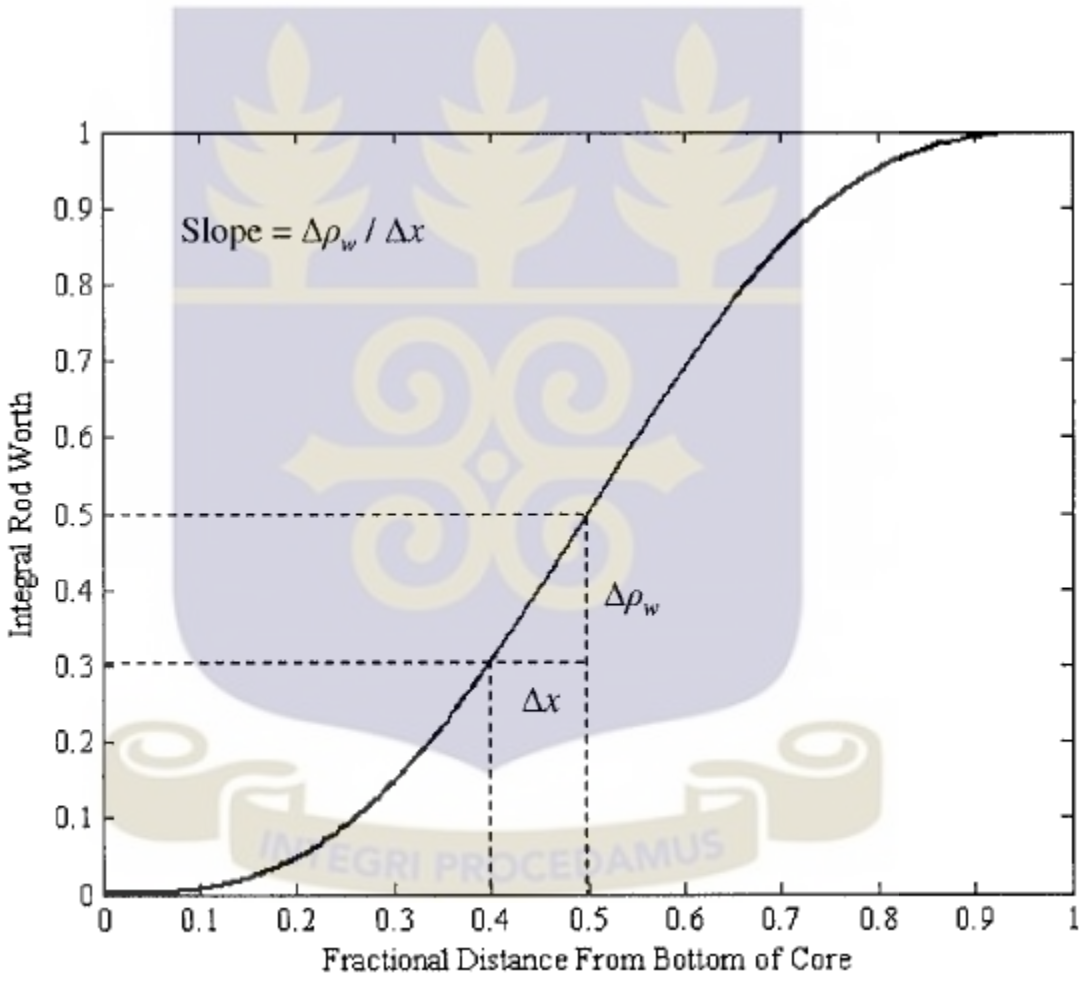

Figure 2.1 Integral control rod worth

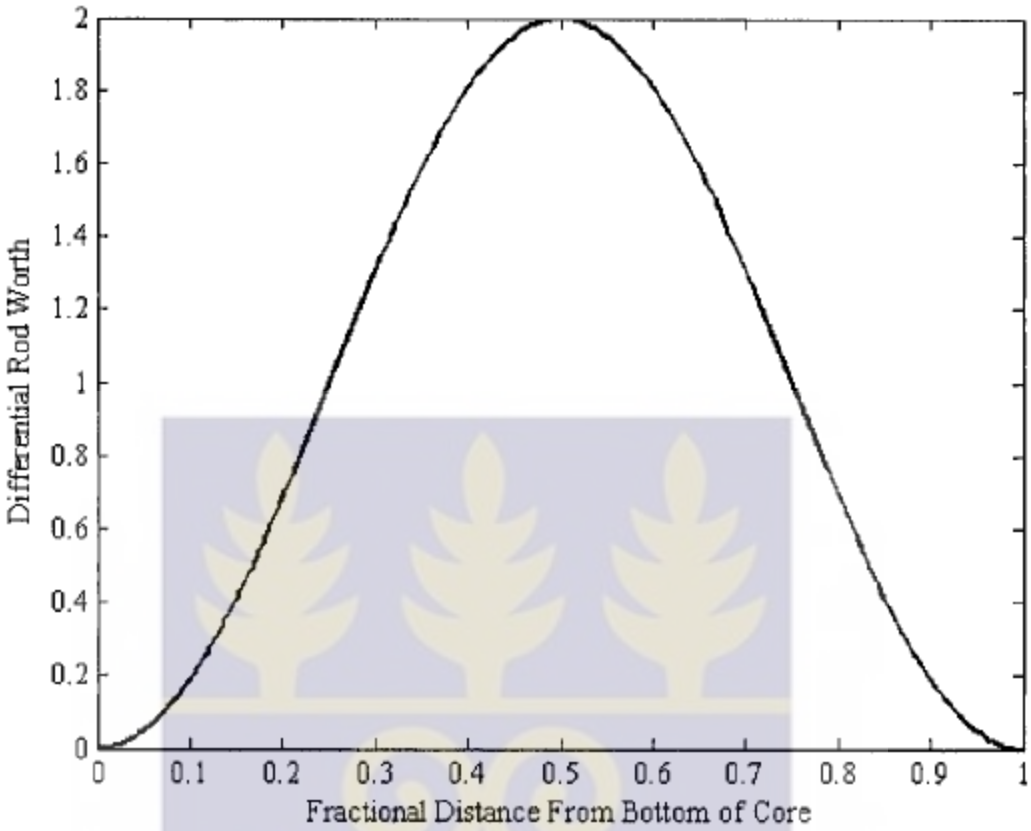

Figure 2.2 Differential control rod worth

2.5 THERMAL HYDRAULICS

2.5.1 Heat Generation and Volumetric Heat Source Determination

The energy released from fission of uranium-235 caused by a thermal neutron is categorized as instantaneous and delayed. Each fission produces about 200 MeV of energy. Instantaneous energy accounts for 93.4 % with a distribution of; kinetic energy of fission fragments (167 Mev), fission neutrons (5 MeV), instantaneous Gamma-ray energy (5 MeV) and capture Gamma-ray Energy (10 MeV). Delayed energy accounts for 11.5% with a distribution of; Beta Particles from Fission Products (7 MeV), Gamma-rays from Fission Products (6 MeV), and Neutrinos (10 Mev).

The efficiency with which reactor components are able to transport the heat from the fuel meat into the coolant is critical in the operation of a reactor. This requires a thorough understanding of the heat distribution within the fuel meat and through the cladding relative to thermal properties of the fuel meant and cladding material.

The rate at which fission and heat production occurs in afuel rodis a function of position and it varies for different fuel rods [35]. The rate of heat production per unit volume at a point $\vec{r}$ is given as;

$$q'''(\vec{r}) = G\sum_f \phi(\vec{r}) \frac{MeV}{cm^3.\sec} \qquad 2.13$$

where $q'''(\vec{r})$ is the volumetric heat source $\left(\frac{MeV}{cm^3.\sec}\right)$, G is the fission energy deposited in the fuel per fission (≅180 MeV/fission) and Σ_f is the macroscopic fission cross section.

In general terms, the flux and cross section are position$(\vec{r})$, energy(E), and time(t) dependent. This relationship is presented by Equation 2.14

$$q'''(\vec{r},E,t) = G\Sigma_f(\vec{r},E,t)\phi(\vec{r},E,t) \qquad 2.14$$

where, the volumetric heat generation rate can be differentiated in terms of energy. For a steady state condition, the volumetric heat generation rate is independent of time but dependent on position.

$$q'''(\vec{r}) = G\int_0^{\infty}\Sigma_f(\vec{r},E)\phi(\vec{r},E)dE \qquad 2.15$$

Considering that in a reactor, neutrons have different energies, the flux is treated as a sum of the various energy group integrals.

$$q'''(\vec{r}) = G\sum_{g=1}^{N_g}\int_{Eg}^{E_{g-1}}\Sigma_f(\vec{r},E)\phi(\vec{r},E)dE \qquad 2.16$$

If the group flux and the average cross sections are redefined, such that the fission rate over the group is preserved,then an approximate relationship would be expressed as Equation 2.17.

$$\int_{Eg}^{E_{g-1}}\Sigma_f(\vec{r},E)\phi(\vec{r},E)dE \equiv \Sigma_{fg}(\vec{r})\phi_g(\vec{r}) \qquad 2.17$$

where the flux average group is

$$\phi_g(\vec{r}) = \int_{E_g}^{E_{g-1}} \phi(\vec{r}, E) dE$$

and from Equation. 2.17, the group average cross section can be written as

$$\Sigma_{fg}(\vec{r}) = \frac{\int_{Eg}^{E_{g-1}} \Sigma_f(\vec{r}, E)\phi(\vec{r}, E)\, dE}{\int_{g}^{E_{g-1}} \phi(\vec{r}, E)\, dE} = \frac{\int_{Eg}^{E_{g-1}} \Sigma_f(\vec{r}, E)\phi(\vec{r}, E)\, dE}{\phi_g(\vec{r})}$$

The volumetric heat generation rate could then be expressed in terms of the averaged group fluxes and group cross sections respectively;

$$q'''(\vec{r}) = G\sum_{g=1}^{N_g} \Sigma_{fg}(\vec{r})\phi_g(\vec{r}) dE \qquad 2.18$$

The spatial dependence of the flux is a function of the geometry and structure of the reactor. A bare, finite cylinder is a good theoretical model for computing heat removal.

$$\phi_T = \frac{3.63P}{E_R \bar{\Sigma}_f V_f} J_o \frac{2.405r}{\tilde{R}} \cos\frac{\pi}{\tilde{H}} \qquad 2.19$$

where P is the total power of the reactor in joules, E_R is the recoverable energy per fission in joules, V_f is the reactor volume in cm^3 , and $\tilde{R}$ and $\tilde{H}$ are its outer dimensions in centimeters to the extrapolated boundaries.

2.5.2 Heat Flow

The removal of heat from the reactor is achieved by conduction and convection which are fundamentally different processes. These are conduction and convection. In conduction, the transmission of heat from one point to another in a media is due to temperature

differences that occur between the two points. There is, however, no macroscopic movement of any portion of the body. This mechanism, governs the transfer of heat generated in the fuel to the surface of the rod.

In convection, heat is transferred from one point into a moving liquid or gas due to difference in temperature and re-ejected at another point. Thus, heat is conducted from the fuel to the surface and then moved into the coolant and eventually out of the system by convection.

Both conduction and convection require a medium in their heat transfers, however heat can also be transferred as thermal radiation across two bodies at different temperatures and separated by a vacuum. This process is of little significance in most reactors except those that are gas cooled [35].

Fourier's law is a fundamental relationship that governs heat conduction. For an isotropic medium it is given as;

$$q'' = -k\,grad\,T \qquad 2.20$$

where q'' is the heat flux $(\frac{W}{m^2})$, k is the thermal conductivity $(\frac{W}{m-K})$, and T is the temperature K.

The heat conduction amongst nuclear elements follows the Fourier field equation described by Equation 2.21. This equation describes how temperature is distributed in a material.

$$\nabla^2 T + \frac{q'''}{k} = \rho c_p \frac{\partial T}{\partial t} \qquad 2.21$$

where T is temperature ($^{\circ}C$), q''' is the source strength or the volumetric heat flux, ρ is the density, c_p is the specific heat, k is the thermal conductivity and t is the time [8].

2.5.3 Temperature Dependence on Power

The study of the dependence of power on temperature through various simulation codes has shown a semi-empirical relationship between the core inlet temperature, the rise in coolant temperature and the power level. Equation 2.22 shows the semi-empirical relationship [17].

$$T = \left(5.725 + 147.6H^{-2.64}\right) T_i^{-0.35} P^{(0.59+0.0019T_i)} \qquad 2.22$$

where; ΔT is Temperature difference between inlet and outlet orifices (^{o}C)

H =Height of the inlet orifice in millimeters

T = inlet temperature (^{o}C)

P = The power of the reactor level (kW)

For GHARR-1 the orifice height H is kept at 6mm to keep the reactor safe. Thus substituting 6 mm for H in Equation 2.22 reduces it to Equation 2.23

$$T = 7.027 T_i^{-0.35} P^{(0.59+0.0019T_i)} \qquad 2.23$$

Introducing the natural log and the exponential operators, Equation 2.23 can be expressed in terms of power as;

$$P = \exp\left[\left(\ln\frac{\Delta T}{7.027T_i^{-0.35}}\right)(0.59+0.0019T_i)^{-1}\right] \quad 2.24$$

From Equation. 2.24, it can be deduced that the relationship between reactor power and coolant temperature is linear. A rise in coolant temperature would cause a corresponding rise in reactor power. Besides this deduction, it is worth noting that thermal hydraulic parameters can be used to determine reactor power.

Neutronic parameters (neutron flux values) can also be used to predict the fission power of the reactor as can be deduced from Equation 2.25. However, these equations are varied as long as nuclear data parameters are accurately predicted or known [19]. Equation 2.25 relates the fission power and the flux;

$$P = 3.1\times10^{10}\Sigma_f V_f \phi \quad 2.25$$

Where ϕ = average neutron flux in the inner irradiation channels ($\frac{cm^2}{s}$)

Σ_f = macroscopic fission cross section of the core fuel given as $1.013x10^2\ cm$

V_f = Volume of the core (cm^3) given as $V_f = \pi r^2 h$

Core height(h) = 23 cm

Core radius (r) = 11.5 cm

The GHARR-1 is cylindrical with a cross section area of $415.47cm^2$ and substituting the various parameters into Equation. (2.25), the power equation reduces to Equation2.26 which is only dependent on the flux (neutronic parameter). This shows the linear relationship between the reactor power and the neutron flux.

$$P = 3.0\times10^{8}\phi \quad 2.26$$

2.5.4 Steady State

A reactor that is operating at constant power is referred to as operating in a steady state mode. For a reactor to operate in a steady state, with a time independent temperature distribution, all the excess heat generated above the steady state condition must be removed promptly by passing a fluid through the core and other areas where heat is generated . The characteristics and behaviour of the coolant system are a crucial consideration in the design of a nuclear reactor [35].

The rate at which heat is removed from the MNSR to maintain a maximum steady state operation time is largely affected by the inlet flow orifice, which in turn determines the temperature effect. Originally the MNSR design had an inlet orifice height of 4.5 mm. This has been increased to 6mm which has made the commercial MNSR to have improved safety features [25].

2.5.5 Transients

The term transient refers to any significant deviation from normal operating conditions of reactor parameters relative to time. These transients are assigned four categories; Very slow transient. A typical example is burn up or depletion with time which occurs with a time constant in years. Slow transients have a time constant in order of hours. The buildup of xenon and samarium is an example of this type of transient. Normal transients have a time constant in seconds with examples such as fuel and moderator temperature change. Fast transients such as the drop in control rod or withdrawn at a maximum rate (in seconds) [36].

The change in neutron flux associated with variation in the material or geometry of a reactor is accounted for as a reactor transient. This type of transient is bound to occur during normal operations due to control rod movement or when the reactor is refueled. Transient responses are more critical when an accident occur as reactor properties change rapidly with large amplitudes. These conditions require a thorough understanding for improved identification, prevention and mitigation of transients. [24].

2.6 BOILING HEAT TRANSFER

Boiling can be understood as the transition from liquid to vapor through a process called nucleation which is formation of bubbles. For nucleation to occur, there should be an increase in heat. The amount of heat required to transition a unit mass liquid into vapor can be expressed using Equation 2.27.

$$h_{fg} = h_g - h_f \tag{2.27}$$

Where h_{fg}, h_g, h_f are the heat required for transition, heat due to the vapor phase and heat due to the liquid phase at saturation and constant pressure.

For a bubble to have mechanical equilibrium (relative to the Young-Laplace equation) in a regime where it is surrounded by a liquid, and where the vapor pressure within the bubble is somewhat higher than the pressure of the liquid around the bubble, the vapor and liquid temperatures must be greater than the saturation temperature (T_{sat}). From the use of the Clausius-Clapeyron equation to relate saturation temperatures and pressures,

the magnitude of the superheat $(T_{nucleate} - T_{sat})$ required to sustain the bubble is inversely proportional to the radius of the bubbles [37].

$$(T_{nucleate} - T_{sat})\alpha\rho c_p \frac{1}{r_{bubble}}$$

2.28 **Pool Boiling**

The heat transfer mechanisms that occur due to boiling can be understood from Figure 2.5. The figure shows a qualitative boiling curve for water on a heated surface at temperature (T_s). It is a plot of the heat flux $\left(q''\left(W/m^2\right)\right)$ against excess heat $\Delta T_{excess} = T_s - T_{sat}$. As the heat is progressively increased in a pool of liquid, the excess temperature also increases.

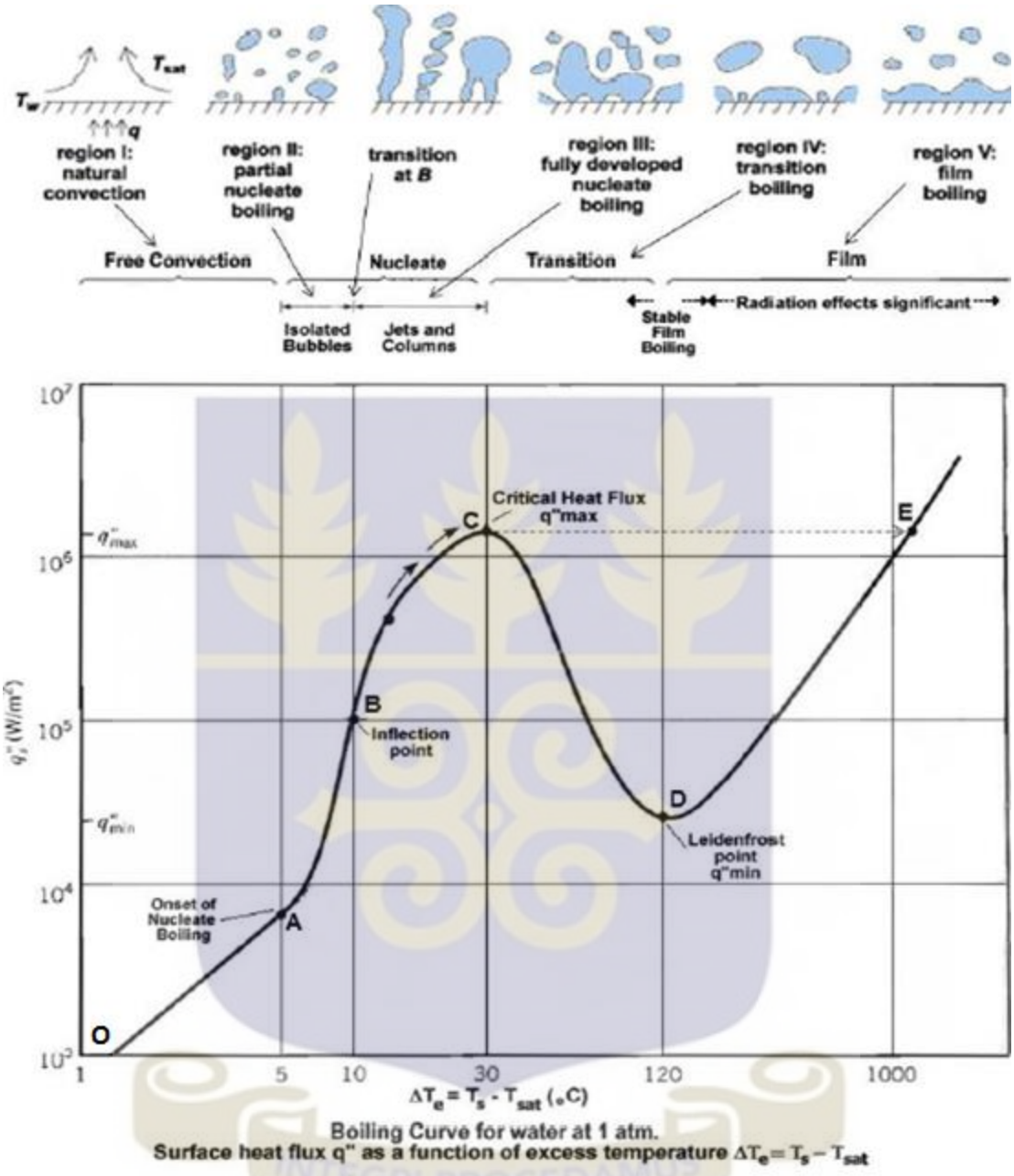

Figure 2.5 Variation of heat flux with surface- liquid temperature difference in pool boiling [38].

2.6.2 Onset of Nucleate Boiling (ONB)

In the region O→A the wall temperature is below T_{sat} as such bubble nucleation cannot be initiated. The heat transfer from the wall is purely by single-phase free convection. However, at point A, the initial bubble appears on the surface. This point is referred to as Onset of Nucleate Boiling (ONB) and the corresponding temperature as ONB temperature.

To avoid boiling excursion, a parameter Onset of Nucleate Boiling ratio (ONBR) is defined to set a temperature operating margin. Equation 2.29 defines the ONBR and the limiting factor in this margin is the temperature difference between the ONB temperature (T_{onb}) and the coolant inlet temperature (T_{inlet}). The variable part is the temperature difference between the surface temperature and the coolant inlet temperature.

$$ONBR = \frac{T_{onb} - T_{inlet}}{T_{surface} - T_{inlet}} \qquad 2.29$$

In region A→B more vapor bubbles form, grow and eventually detach from the wall due to the buoyancy effect. This heat transfer regime is called nucleate boiling. The steep gradient of the heat flux in this region is due to mixing of the fluid as a result of bubble motion. As the temperature increases bubbles become unstable with a lot of mixing near the wall which increases the heat transfer. As such, nucleate boiling is a much more effective mechanism for heat transfer than free convection.

2.6.3 Departure from Nucleate Boiling Ratio

Region B→C is characterized with a lot of dense bubbles at the surface which coalesce and form a continuous vapor film. In this region, there is a quick change from nucleate boiling to film boiling. This abrupt change is referred to as Departure from Nucleate Boiling (DNB), Critical Heat Flux (CHF), burnout, or boiling crisis.

To avoid film boiling excursion an operational safety limit DNBR is defined as described by Equation 2.30. In water cooled nuclear reactors, the DNBR is estimated by the heat flux. During normal operations, fluctuations do occur and they tend to cause variations in the DNBR and may reduce the safety margins [17, 29].

Heat removal in GHARR-1 is dependent on the upper and lower orifice heights which were determined to ensure effective cooling of the core. The criteria of thermal-hydraulic design require that the burnout ratio or DNBR should be larger than the calculated burnout heat flux i.e. DNBR> 2.5 [29].

$$DNBR = \frac{q''_{critical}}{q''_{actual}} \qquad 2.30$$

where $q''_{critical}\left(\frac{MW}{m^2}\right)$ = heat flux at the departure from nucleate boiling

$q''_{actual}\left(\frac{MW}{m^2}\right)$ = heat flux relative to the prevailing power.

For GHARR-1, with low velocity flow, the Mirshak correlation is employed to calculate the $q''_{critical}$ and is given as DNB. In subcooled boiling, $q''_{critical}$ is a function of the coolant velocity, the degree of subcooling and pressure [17].

$$q''_{critical} = 1.5\times10^{6}\left(1+0.1107u\right)\left[1+9.14\times10^{-3}\left(\Delta T\right)\right]\left(1+1.89\times10^{-1}\Psi\right) \qquad 2.31$$

where $u = 1.2727\dfrac{\dot{m}}{\rho_{cool}H^{2}}$ which is the coolant velocity in the range

Ψ = pressure [MPa]

If heat flow parallel to the fuel or channel can be ignored, the actual heat flux can be describe by Equation 2.32

$$q''_{actual} = \frac{q'''A_f}{C_c} \quad 2.32$$

where q''' is the heat production per unit volume, A_f is the cross-sectional area of the fuel, and C_c is the circumference of a heated rod. Parameters for GHARR 1 describe in Equation 2.32 are provided in Appendix E.

In region C→D the film become unstable and spread over the surface. This results in a reduction in both the heat flux and the heat transfer coefficient because vapor is a poor heat conductor. Point D is called the Leiden frost point which gives the minimum heat flux.

Region D→E represents an increase in heat flux due to the surface being covered with vapour. The steep slope shows the rapid change in temperature to point E where the temperature is well above the CHF temperature but having relatively the same heat flux. For normal operation of a reactor, the heat fluxes must be well below the CHF. This limit is imposed by the CHFR described above by Equation 2.30 [28].

2.6.4 Flow Instability Power Ratio (FIR)

The coolant's ability to remove heat from the reactor is important for safety of a nuclear reactor. This is done by ensuring the coolant flow is stable within the flow channels. Stability of coolant flow can be affected by factors such as surface roughness, onset of nucleate boiling among others. For a smooth surface, the ONB can be a major source of flow instability as the formation of bubbles on the surface of the channel can act as surface roughness which may cause flow instability [39].

The PLTEMP/ANL code which has been used in this work for steady state analysis uses, for its routine checks, the Babelli-Ishii criterion for excursive flow instability after boiling. The criterion is based on the Subcooling number and the Zuber number which are described by Equations 2.34 and 2.35

$$\frac{N_{sub}}{N_{zub}} = \frac{L_{nvg}}{L} + \frac{A_F}{\zeta_H L}\begin{cases} 0.0022 P_e if P_e < 70,000 \\ 154 if P_e > 70,000 \end{cases} \quad 2.33$$

where

$$N_{sub} = \frac{\Delta h_{in}\left(\rho_{f,nvg} - \rho_{g,nvg}\right)}{h_{fg}\rho_{g,nvg}} \quad 2.34$$

$$N_{zub} = \frac{q''_w \zeta_H L\left(\rho_{f,nvg} - \rho_{g,nvg}\right)}{\rho_{in} A_F V_{in} h_{fg}\rho_{g,nvg}} \quad 2.35$$

$$\frac{N_{sub}}{N_{zub}} = \frac{\Delta h_{in}\rho_{in} A_F V_{in}}{q''_w \zeta_H L} \quad 2.36$$

Δh_{in} = Subcooling at the start of heated length, J/kg = $h_f\left(P_{in}\right) - h_{in} \approx h_f$ (Pnvg) - h_{in}

Δh_{nvg} = Subcooling at the NVG position, J/kg = $h_f\left(P_{in}\right) - h_{nvg} \approx h_f\left(P_{nvg}\right)$ - h_{nvg}

L = Channel heated length, m

L_{nvg} = Non-boiling length, i.e., the distance from the start of heated length of channel to the position of net vapor generation, m

$\frac{L_{nvg}}{L}$ = Dimensionless non-boiling length

$\left(\frac{L_{nvg}}{L}\right)_{critical}$ =Dimensionless non-boiling length critical value based on experimental data

A_F = Flow area of channel, $\left(m^2\right)$

ζ_H = Heated perimeter of channel, $\left(m\right)$

ρ_{in} = Coolant density at inlet, $\left(kg/m^3\right)$

V_{in} = Coolant velocity at inlet, $\left(m/s\right)$

q''_w = Wall heat flux, $\left(W/m^2\right)$

P_e = Peclet number = $\rho in\ CpVinDh/K$

For flow to be stable, the RHS in Equation 2.33 should be greater than the LHS. The coolant inlet velocity at which the equation turns from unstable to stable is taken to be the velocity at Onset of Flow Instability (OFI). The inlet velocity and the flow rate at OFI can be calculated from the exit coolant temperature Tout using Equation 2.37.

$$\rho_{in}A_F V_{in} = w = \frac{Q}{h\left(P_{out},T_{out}\right)-h\left(P_{in},T_{in}\right)} \qquad 2.37$$

This equation is obtained by equating the total power to the coolant enthalpy change multiplied by the flow rate. The exit temperature $\left(T_{out}\right)$ can then be obtained from the ratio

$$r = \frac{T_{sat,out} - T_{out}}{T_{out} - T_{in}} \qquad 2.38$$

where r is the ratio at onset of flow instability (OFI).

The simplified Babelli-Ishii criterion for flow instability due to onset of boiling is described by Equation 2.39

$$\frac{N_{sub}}{N_{zu}} = \begin{cases} > 1.36 \ \ clearly\ stable \\ < 1.36\ to\ 1.0 \ \ maybe\ stable\ or\ unstable \\ < 1.0\ clearly\ unstable \end{cases} \qquad 2.39$$

2.7 SIMULATION MODELS

Models and Simulations are used to provide a representation of a system so that its behaviour can be studied. A Model is defined as a product of a system which can be physical or digital, where as a Simulation is an application of a Model to study the behaviour of a system. Simulations and Models help in studying the behaviour of systems with the flexibility of varying a wide range of parameters that are otherwise difficult or impossible to vary on a physical system.

Nuclear reactors are complex systems with a lot of mechanical, neutronics, and thermal-hydraulic properties that require extensive studies to ensure safe operation. Most of the parameters associated with these properties are hard to study experimentally as they require changing various components of the reactor core. A number of simulation codes have been developed over the years to help in studying the behaviour of reactors under relative to changes in some of the parameters and materials.

2.7.1 Pin Cell Model

This is a simplified MCNP model of a reactor in which the core is treated as a single fuel rod immersed in an infinite medium of the moderator as shown in figure 2.0. Region "A" represents an aggregate of all fuel material in the core and it is surrounded by an aggregate of the moderator material represented by region B.

Advantages

- Analysis based on the pin cell Model gives an idea of the importance of different contributions to the Reactor Temperature Coefficients

- It is very useful in determining sources of discrepancy between different codes and data libraries.
- It is simple to model as it does not require a detailed surface card.
- It minimizes errors associated with modelling such as input of wrong figures.

Disadvantages

- Simplification of the core entails, certain details are over looked which may have an effect on the results obtained.

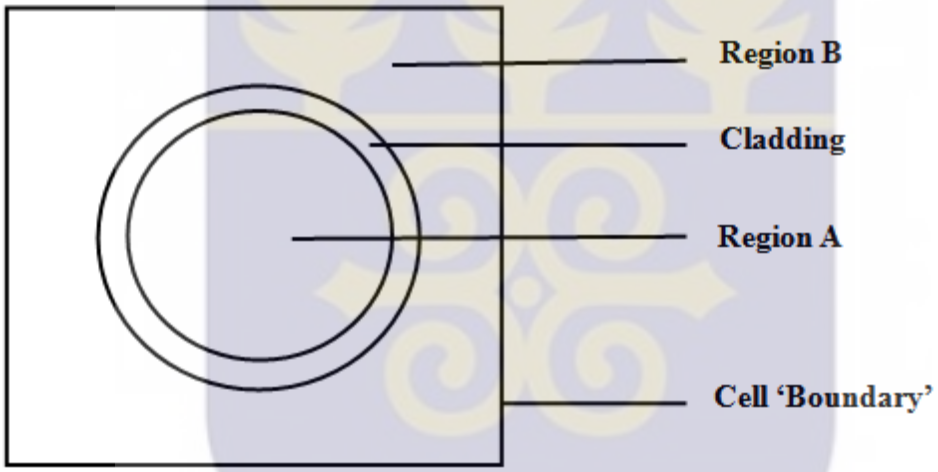

Figure 2.6 Pin Cell model of the reactor core

2.7.2 Full Model Method

The reactor core is modeled with all the structures and components assigned respective cell cards, material cards and surface cards respectively. The model gives all necessary details to reproduce a "system" that is close to the physical reactor core.

Advantages

- It increases the accuracy of predicting the behaviour of the neutron in the core as all materials are modelled.
- It limits the number of parameters needed for modeling before considering the whole reactor
- Available computer memory is not a major concern when analyzing such simple models

Disadvantages

- It is laborious and time consuming
- Has a high potential of making mistakes in modelling numerous parts of the core.

CHAPTER THREE

METHODOLOGY

3.1 MATERIALS AND METHODS/ METHODOLOGY

3.1.1 Simulation Process

Figure 3.1 shows the interplay of the four (4) codes that have been used to simulate fuel depletion, nuclear processes, slow and fast transients, and steady state thermal-hydraulic characteristics of GHARR-1.

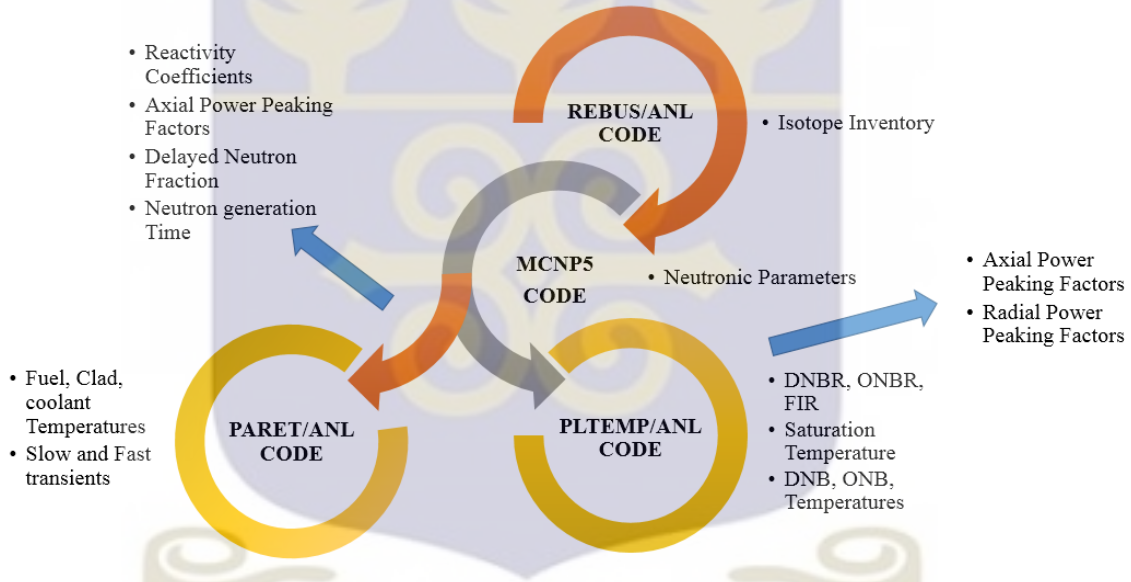

Figure 3.1 Simulation progression for REBUS/ANL, MCNP5, PARET/ANL and PLTEMP/ANL.

3.1.2 REBUS/ANL Code

The REactor BUrnup System code (REBUS/ANL) developed by Argonne National Laboratory (ANL) has evolved away from its roots as a design tool for fast reactors to encompass the needs of thermal reactor design and analysis. Since its conception in the 1960's, REBUS/ANL has always been a general-purpose tool. It was originally designed and coded for capabilities of large main-frame computers, some of which had "small core memory" and others had "large core memory" [40].

3.1.3 REBUS/ANL simulation

The REBUS/ANL was used in this work to determine the isotopic densities of fission products in the fuel due to fuel burnup after nineteen (19)years of operation. It was used as a choice code for this work because it has provision for the user to specify the types of isotopes to be tracked.

The code was run under the current operation scheme of GHARR-1 for2.5 hours per day, 4 days a week and 52 weeks a year. This was done to produce an isotope inventory that reflects the actual operations of GHARR-1.

The output of the code provided the isotopes that were required along with LUMP and DUMPED isotopic densities. The LUMP and DUMPED mass values were processed manually to include isotopes that were considered significant. The choice of isotopes that were processed to be included to the fission products was made based on two parameters;

the fission yield and their cross sections. The LUMP and DUMPED were assigned isotopes, because MCNP5 had no provision for library of LUMP and DUMPED isotopes but could use specified isotopes of which MNCP has libraries.

The isotopic densities that were generated from the REBUS/ANL code were used to update the fuel material card m6 in the MCNP model for GHARR-1. A list of isotopes obtained from REBUS/ANL code is provided in Appendix A.

3.1.4 MCNP Code

Monte Carlo N-Particle Transport Code (MCNP) is a software package for simulating nuclear processes. It is developed by Los Alamos National Laboratory since at least 1957 with several further major improvements. It is used primarily for simulation of nuclear processes, such as fission, but has capability to simulate particle interactions involving neutrons, photons, and electrons.

The MCNP code is particularly useful for complex problems that cannot be modeled by computer codes that use deterministic methods. The individual probabilistic events that comprise a process are simulated sequentially. The probability distributions governing these events are statistically sampled to describe the total phenomenon. It consists of following each of many particles from a source throughout its life to its death in some terminal category (absorption, escape, etc.). Probability distributions are randomly sampled using transport data to determine the outcome at each step of its life.

MCNP was used because of its ability to model complex three-dimensional geometries and its extensive validation [25].

3.1.5 MCNP Simulation Criticality Problem

Criticality problems in MCNP are simulated using the KCODE card which requires the nominal number of source histories (N) per $cycle$, an initial guess of k_{eff} ,the number of source cycles,(I_c),to skip before k_{eff} accumulation, active number of cycles(I_A),and the total number of cycles(I_t) [32].

The control rod worth, delayed neutron fraction, neutron generation time, shutdown margin, and power peaking factor cases were simulated with the following specifications in the model; N was set at 300,000, k_{eff} was given an initial guess of 1.004, I_t was set as 250 cycles with the first 20 cycles I_c being inactive and the 230 cycles being active. These values were sufficient to provide sufficient statistical accuracy in the results. The value for the number of cycles to be skipped was chosen to provide sufficient cycles for k_{eff} to statistically converge around a certain solution, allowing for the most accurate results to be obtained. The initial guess of 1.004 was sufficient to allow for good statistical accuracy in the prediction. A total of 69 million particles were used for each simulation.

Reactivity coefficients were simulated using the following specifications in the model; N was set at 200,000, k_{eff} was given an initial guess of 1.004, I_t was set at 220 cycles with

the first 20 cycles I_c being inactive and the 200 cycles I_A being active. A total of 40 million particle histories were used.

A total of 48 simulations were used to predict the neutronics and kinetic parameters.

3.1.6 Irradiated Core Model

Due to fuel burnup, the clean core model for GHARR-1 was modified to reflect the current status after nineteen (19) years of operation. An inventory of fission products obtained from REBUS/ANL code and presented in Appendix A were used to update the material card m6 in the MCNP5 model of GHARR-1. The m6 card provides information on the composition of the fuel in the core.

A 9 mm layer of beryllium was added to the top shim tray to compensate for the loss in excess reactivity due to fuel burnup. Figure 3.2 shows the layer of beryllium added to the top shim tray.

This model of GHARR-1 was used for all simulation that involves the irradiated core.

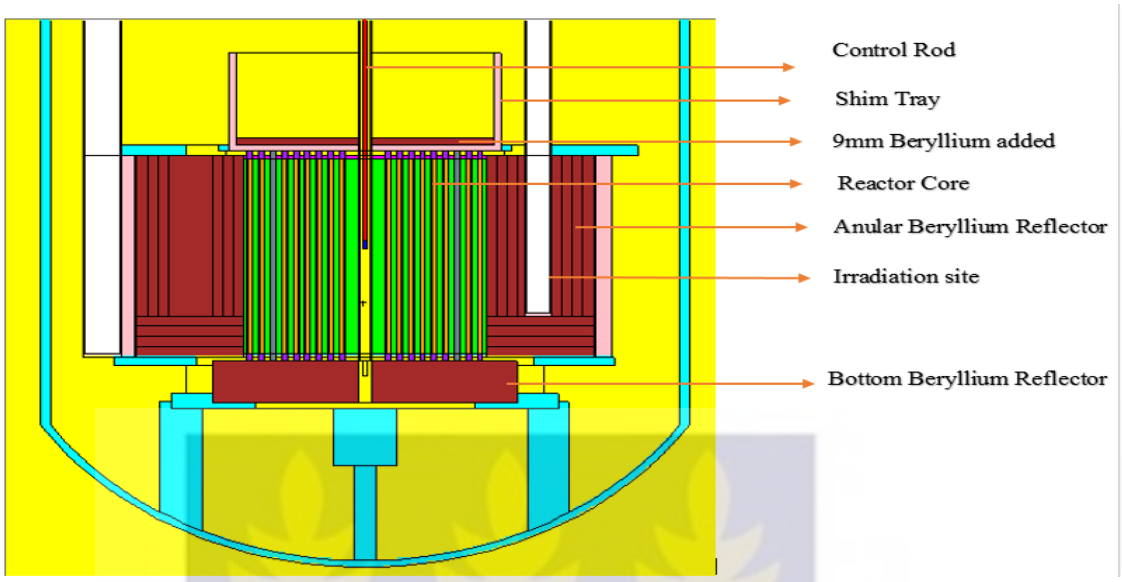

Figure 3.2MCNP visual editor X vertical cross section for GHARR-1 with 9 mm of beryllium added to the top shim tray

3.1.7 Excess Reactivity

The core was simulated with the control rod fully withdrawn. With the KCODE card parameters set as described in Section 3.1.5. The eigenvalue obtained was used to compute the excess reactivity using Equation 2.2.

3.1.8 Control Rod Worth

Two cases were simulated for the model, with KCODE parameters set as described under in section3.1.5. The simulation for the first case was carried out with the control rod fully withdrawn, and the eigenvalue obtained was designated as k_{out}. The simulation for the second case involve a model in which the control rod was fully inserted into the reactor

core and the eigenvalue obtained was designated as k_{in}. The two eigenvalues k_{out} and k_{in} were employed to compute the control rod worth using Equation 2.6

3.1.9 Reactivity Coefficients

3.1.9.1 Moderator Temperature Coefficient

Analysis of moderator temperature reactivity coefficient was done by changing the temperature corresponding equilibrium energy on card TMP and the temperature corresponding density in all Cell cards that contain water in the model. The eigenvalues were predicted for the temperature range 20 to 100 $^{\circ}C$ Table 3.2 shows the relationships of temperature to equilibrium temperature and densities that were used. The reactivity obtained from the eigenvalues were plotted against temperature. The relationship between temperature and reactivity was determined using the 3rd order polynomial equation. Equation 3.0 was used to compute the moderator temperature coefficient.

$$\alpha_x = \frac{\partial \rho}{\partial x} \qquad 3.0$$

Where α_x is the reactivity coefficient for parameter χ

The Moderator temperature was analysed with the density for the water unchanged. Only the temperature for the water on the TMP card was change. The relationship between temperature and reactivity was determined using 2nd order differential equation.

3.1.9.2 Moderator Void coefficient

The coolant density (voiding) was perturbed in the MCNP model. The densities that were used were corresponding to temperatures range 20 °C to100 °C. Table 3.2 shows the relationship between the temperature, equilibrium energy, and the void. The reactivity for each eigenvalue were plotted against the corresponding temperature. The relationship between temperature and reactivity was determined using the 4nd order polynomial equation. Equation 3.0 was used to compute the moderator void coefficient.

3.1.9.3 Fuel temperature coefficient

The Model was altered by changing the TMP data card in the model to represent the desired temperature. The changes that were made to the TMP data card corresponded to the equilibrium energy of the atoms in the fuel at that temperature. The temperature range 30°Cto 600 °C was used for the MCNP runs to predict the corresponding eigenvalues. A summary of the various parameters that were changed in the MCNP input deck for predicting the multiplication factors corresponding to different temperatures, densities and percent void is presented in Table 3.1 below. Table 3.2 shows the relationship between temperature (°C) and the corresponding equilibrium temperature (MeV) that were used in the model.

Table 3.1 Parameter changes to MCNP input deck for reactivity coefficient analysis

Reactivity coefficient	Temperature Range (°C)	Fuel Temperature	Core Water Temperature	Fuel Density	Core Water Density
Fuel	20-800	Corrected to	unchanged	unchanged	unchanged

Temperature		temperature			
Moderator Temperature	20-100	unchanged	Corrected to temperature	unchanged	Corrected to temperature
Void	20-100	unchanged	unchanged	unchanged	represent void

Table 3.2 Relationship between Temperature, Equilibrium Energy Density and Percent Void.

Temperature (°C)	Equilibrium energy (MeV)	Density (g/cm3)	Void (%)
20	2.5125e-08	0.99820	0
30	2.6124e-08	0.99567	0.18
40	2.6935e-08	0.99221	0.7
50	2.7847e-08	0.98807	1.02
60	2.8709e-08	0.98324	1.5
70	2.9571e-08	0.97777	2.00
80	3.0432e-08	0.97170	2.55
100	3.2156e-08	0.95835	3.91

3.1.10 Kinetic Parameters

3.1.10.1 Delayed Neutron Fraction

The effective delayed neutron fraction was predicted using the Prompt method which requires two cases to predict eigenvalues; in the first case, the eigenvalue for prompt neutrons k_p only was predicted and in the second case, the eigenvalue k_c combining prompt and delayed neutrons was predicted.

The TOTNU data card with entry NO was used to obtain the eigenvalue for prompt neutrons only. The TOTNU data card with entry NO prevents the influence of delayed neutrons and thus the multiplicity per fission is due to the average prompt neutron and subsequently k_p is computed for all fissionable nuclides with prompt values available.

The TOTNU card without any entry after it was used to predict the total average number of neutrons from fission. This takes into account both prompt and delayed neutrons and thus the total effective multiplication factor k_{eff} was calculated.

The values for k_p and the k_{eff} obtained were used to compute the delayed neutron fraction using Equation 3.1

$$\beta_{eff} = \frac{1-k_p}{k_{eff}} \qquad 3.1$$

3.1.10.2 Neutron Generation time

The neutron generation time was predicted using the $1/V$ absorber method. In this method, all materials in the core are doped with a small amount of a $1/V$ absorber material. Different concentrations of the doping material are used. The corresponding perturbed eigenvalue for each concentration is given as k_{pt} and the steady state unperturbed eigenvalue is given as k_u.

The $1/V$ absorber material inserts a negative reactivity which is given as

$$\rho = -\frac{\Delta k}{k} = \frac{k_u - k_{pt}}{k_u * k_{pt}} \qquad 3.2$$

According to Bretscher [42, 45], the negative reactivity inserted can be expressed by Equation 3.3.

$$-\frac{\Delta k}{k} = l_p V n \sigma \text{ thus } l_p = \frac{-\frac{\Delta k}{k}}{V n \sigma} \qquad 3.3$$

where l_p is the neutron lifetime,

n is the atomic density of the $1/V$ absorber (atoms/b-cm)

V is the speed of thermal neutrons = 2.2E5 cm/s

σ is the absorption cross section of the absorber (B-10) =3837b

The neutron generation time is given as

$$\Lambda = \lim_{n \to 0} l_p = \lim_{n \to 0} \frac{-\frac{\Delta k}{k}}{V n \sigma} \qquad 3.4$$

In this work, boron-10 was used as the doping material because of its 1/V neutron absorption property. The materials were doped with 5 different concentrations ranging from $6.0\times10^{-8}-15\times10^{-8}$ atoms/b-cm in increments of 1.0×10^{-8} atoms/b-cm. For each concentration, the KCODE data card, with parameters set as described in Section 3.1.5, was used to simulate the eigenvalue k_{pt}.The corresponding negative reactivity inserted and the prompt neutron lives were computed using Equations 3.2 and 3.3.

To determine the neutron generation time Λ, values obtained for neutron life time l_p from Equation 3.3 were plotted against their corresponding $1/V$ absorber concentrations. The graphical application of Equation 3.4 was used to determine the neutron generation time which is the intercept on the Y-axis when the graph is extrapolated backwards.

3.1.11 Thermal Hydraulics

3.1.11.1 Transient Analysis

The transient studies of GHARR-1 after nineteen (19) years of operation were studied using the Program for Analysis of REactor Transients (PARET/ANL) code (Version 7.3 of 2007). The PARET/ANL Code was initially developed for analysis of the SPERT-III experiments for temperatures and pressures typical of power reactors [42]. Modifications have been made to the code to incorporate reactor thermal–hydraulic analysis; these include departure from nucleate boiling, flow instability, single and two-phase heat transfer correlations, and flow rates encountered in research reactors. It also gives an estimate of voiding produced by subcooled boiling through its optional voiding model.

The code has the capability to provide a coupled thermal–hydraulic and point kinetics with continuous reactivity feedback [13,42].

The conservation equations used in the model is given by three equations expressed as;

$$\frac{\partial \bar{\rho}}{\partial t} = \frac{\partial G}{\partial z} \tag{3.5}$$

$$\frac{\partial G}{\partial t} + \frac{\partial}{\partial t}\left(\frac{1G^2}{\rho'}\right) = \frac{\partial P}{\partial z} - \left(\frac{f}{\rho}\right)\left(\frac{|G|G^2}{2D_e}\right) - \bar{\rho}g \tag{3.6}$$

$$\rho'' \frac{\partial E}{\partial t} + G\frac{\partial E}{\partial z} = q \tag{3.7}$$

where $\bar{\rho} = \rho_l(1-\alpha) + \rho_v$ is the average density

$\frac{1}{\rho''} = \left(\frac{(1-\chi)^2}{\rho_l(1-\alpha)}\right) + \frac{\chi^2}{\rho_v \alpha}$ is the momentum density

$\rho'' = \left[\rho_l \chi + \rho_v(1+\chi)\right]\frac{\partial \alpha}{\partial \chi}$ is the slip flow density

$\rho_v, \rho_l, \chi, \alpha$ are; saturated vapor and liquid densities, vapor weight fraction and vapor volume fraction respectively

G is mass flow rate, P is pressure; E is enthalpy, f is friction factor, g is gravitational acceleration, and q is heat

Changes were made to the clean core input deck model of GHARR-1. Kinetic parameters obtained from MCNP simulations of GHARR-1 after 19 years of operation were used in the model. The cards that were changed and the corresponding parameters are described in Table 3.3.

Table 3.3 Table of Neutronic and Kinetic Parameters used in the PARET/ANL model

PARET card Code	**Pneumonic**	**Parameter and Description**
1005	BBEFF	Delayed neutron fraction
	EL	Prompt neutron generation time
1006	TRANST	Total time investigated for the transient (s)
	GAMMA-0	Constant in fuel temperature feedback equation [$]
1007	GAMMA-1	Linear coefficient in fuel temperature feedback equation [$/T]
	GAMMA-2	Quadratic coefficient in fuel temperature feedback equation [$/T^2]
	GAMMA-3	Cubic coefficient in fuel temperature feedback equation [$/T^3]
	GAMMA-4	Temperature offset coefficient in fuel temperature feedback equation. [$/T^4]
5102-5122	PFQ	Ratio of the hottest channel heat flux axial node to the core-average neutron flux
5202-5222	PFQ	Ratio of the average channel axial node to the core-average neutron flux
9003-9004	REACC	Reactivity at time (s)

The core was simulated for transients with reactivity insertions of 2.1 mk, 3.0 mk, 4.0 mk, 5.0 mk and 6.7 mk. These values were chosen for comparison's sake, with those used in the SAR and other literature relating to GHARR-1.

The model for GHARR-1 was also simulated for the stead state analysis with power of 15 kW and 30 kW. This was accomplished by making changes to the operation code IPROP from the operator specified reactivity mode 1 to power specified operation mode 0. The card 6000 was omitted as a result of selecting the power specified operation mode.

3.1.11.2 Fast Transients

From the neutronics results, the excess reactivity was predicted to be 3.86 mk. An accident was postulated in which the excess reactivity was inserted into the core. The reactivity insertion was analysed for a time steps of 0.5 s which is a standard time for analysis of fast transients [20]. The input on card 1113 were set as; 1.016 m/s for control rod rate of withdrawal, 0.015 s for time delay before control rod movement, 1.0 MW for overpower trip point, 0.0 % for low flow trip point and the, 0.03 MW for initial power.

The first pair REACC and TBL entry on card 9000 was set as 0.0, the third and fourth were set with the same reactivity insertion $ 0.47216 (3.86 mk) but different time steps of 0.5 s and 10.0s respectively.

3.1.11.3 Steady State Analysis

The PLate TEMPerature (PLTEMP/ANL) code was used to study the steady state thermal hydraulics parameters of GHARR-1.

The input deck used was a modification of the one provided in the spectrum of Core Conversion Coordinated Research Project of the International Atomic Energy Agency

(IAEA) and developed at the ANL for testing the application of the code on analysis of the steady state parameters of GHARR-1. The cards that were modified are presented in Table 3.4.

The core of GHARR-1 was modeled for all the 344 fuel pins. The fuel pins were arranged in 12 fuel bundles, with the first 11 bundles containing 30 fuel pins, accounting for 330 fuel pins and the remaining 14 fuel pins were put in the last 12^{th} bundle.

The 0303 card which represents the axil power peaking factor per assembly was updated with the maximum power peaking factor value (FZ). This value was repeated 30 (NELFI) times. The power shape corresponding to FZ was input on the 21 heat transfer nodes on card 0701with each J^{th} node having a relative distance of 0.010952 m from the coolant inlet to the assembly.

The 0309 card was updated with radial power peaking factors. A detailed input deck indication these parameters is presented in Appendix D. Both the axial and radial power peaking factors where obtained from the MCNP simulations of the irradiated core.

A preliminary run was performed for the updated input deck. However, the code could not converge and as such, the inner iteration factor (EPSLNI) on card 0500 was decreased from 0.06 to 0.02. With this change, the simulation was able to converge.

The code was simulated for both the 15kW and 30 kW power to study the steady state parameters of GHARR-1and the results are presented in the next Chapter.

CHAPTER FOUR

RESULTS AND DISCUSSION

The main objective of this work was to evaluate the safety parameters of GHARR-1 after nineteen (19) years of operation. Both neutronic and thermal-hydraulic safety parameters have been evaluated and compared with those provided in the Safety Analysis Report (SAR) [25] and in other literature. The thermal hydraulic parameters were studied for both the steady and transients states of the reactor.

4.0 Neutronic Parameters

Neutronic parameters for GHARR-1 after 19 years of operation were observed to be in good agreement with those provided for in the SAR [25] and in literature. Table 4.1 compares parameters obtained from this work and those provided for in the SAR [25] of GHARR1.

The excess reactivity was predicted to be within the expected margin of 3.5 mk to 4.0 mk. The value for the excess reactivity was predicted to be less than the limiting value of $1/2\beta_{eff}$ .The control rod worth was predicted to be higher than the value for the clean core even though the two values are fairly in agreement. The control rod worth is an important design parameter for the safety of a reactor.

The shutdown margin was predicted to be slightly higher than that provided in [25]. The marked difference could be attributed to errors in simulation and modelling.

Table 4.1 Comparison of Neutronic Parameters from this work and the SAR

Simulation Results	Irradiated Core	Sigma	Safety Analysis Report (SAR) [25]
Control rod fully withdrawn	1.00388	0.00014	1.00400
Excess reactivity (mk)	3.86	-	4.0
Control rod fully Inserted	0.99689	0.00014	-
Control rod worth	6.98	0.02	6.8
Shutdown Margin	3.12	0.08	3.0
Delayed Neutron Fraction ($\Delta k / k$)	8.17507×10^{-3}	4.0×10^{-4}	8.08×10^{-3}
Neutron Generation time ($\Delta k / k$)	8.147×10^{-5}	2.0×10^{-6}	8.12×10^{-5}

The delayed neutron fraction was predicted to be in good agreement with the value provided in [25] despite being higher. A good prediction of the delayed neutron fraction is important when coupling neutronics and thermal hydraulics (that require the use of PARET/ANL) as the value predicted will be used to convert reactivity into dollars.

The neutron generation time is also critical in the computation of the thermal hydraulics parameters.

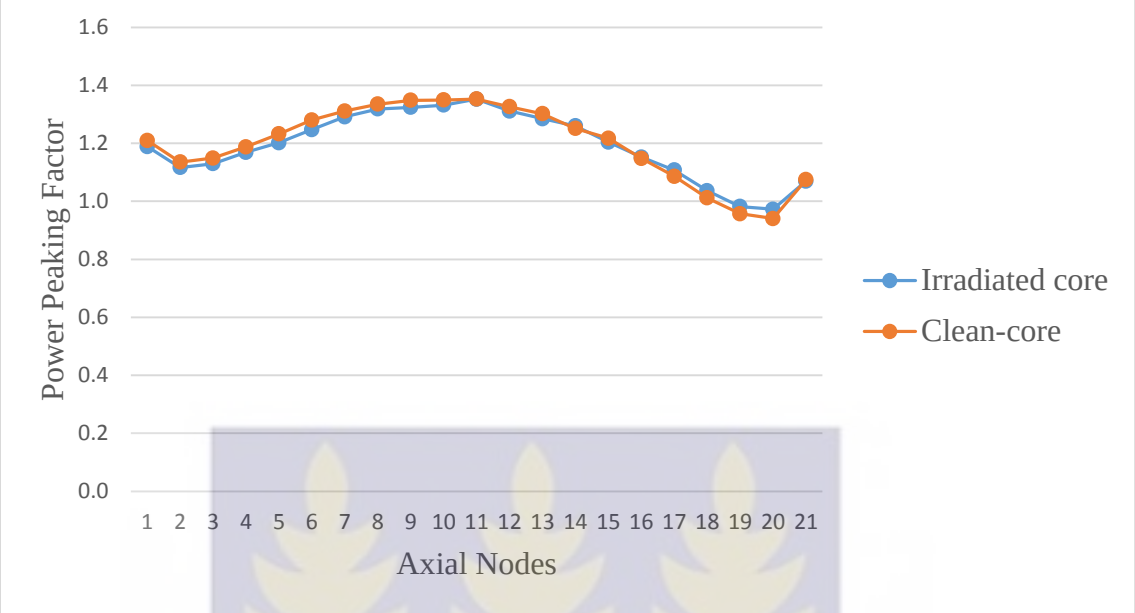

Figure.4.1. Comparison of Axial Power Distribution of the Irradiated and Clean Cores.

Figure 4.1 compares the axial power density distribution of the irradiated core and that of the clean core. The axial power density distribution has its maximum value at the center of the core. This is as a result of the presence of water as moderator when the control rod is fully withdrawn and also the effect of the surrounding beryllium which is maximum around the center. As can be observed, the neutron density starts decreasing axially until it reaches the beryllium reflector where it starts increasing again. The increase in neutron density is due to the presence of beryllium which reflects neutrons into the core. The distribution tilts lower towards the top of the core for both models. This is attributed to the higher leakage of neutron at the top because of the top not being heavily reflected with beryllium like the bottom and the annular directions.

Both the irradiated core and the clean core models show a similar neutron density profile. However, for the first part, the neutron density distribution for the irradiated core is lower compared to that of the clean core. Towards the top of the core, there is an overlap where the irradiated core has a higher neutron density distribution. The lower distribution observed near the bottom of the core for the irradiated core can be attributed to the dominance of fission products in the irradiated core which are not present in the clean core. Some of the fission products have a high absorption cross section for neutrons. The overlap towards the top of the core could be attributed to increased neutron density due to the presence of the 9 mm of beryllium that was added to the top shim tray.

The maximum power peaking factor for the irradiated core was predicted to be 1.3522 and that for the clean core was predicted to be 1.3525. Both values are within the expected range or 1.3-1.5 for light water moderated research reactors.

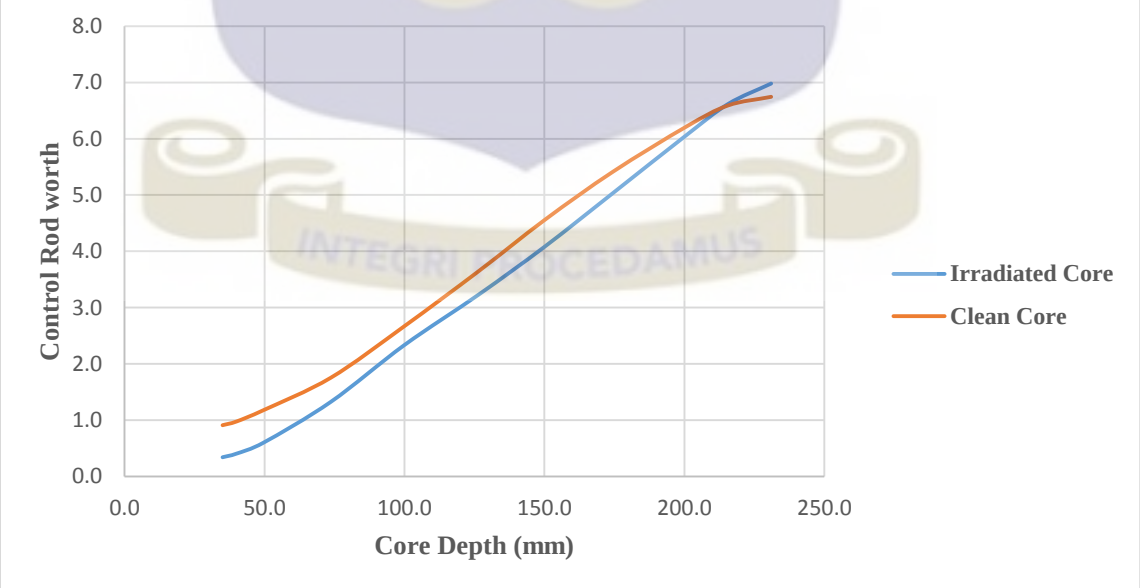

Fig.4.2. Comparison of the Integral control rod for the irradiated and clean cores.

Figure 4.2 compares the integral control rod worth of the irradiated and clean core models. The control rod worth takes the same trend as that observed in Figure 4.1. The curve for the irradiated core is lower compared to that of the clean core for the lower part of the curve. There is, however, an overlap towards the top of the curve. The effect is the same as that explained for the neutron density above. The integral control rod is an important design feature which shows how efficient the control rod is in absorbing neutrons.

Figure 4.3 shows a plot of the neutron lifetime against boron-10 concentration. This plot was extrapolated backwards to zero concentration of boron. The intercept on the neutron lifetime axis gives the value for the neutron generation time. The mathematical computation is elaborated in Equations 3.2 to 3.4. Concentrations of boron lower than 6×10^{-8} atoms/b-cm where not used for the plot as they did not provide significant change in the reactivity value to be used for calculations. This effects of lower concentrations of boron on reactivity which causes the neutron lifetime values to be skewed from linearity is also reported by Hanson A. L and Diamond D. J. [44].

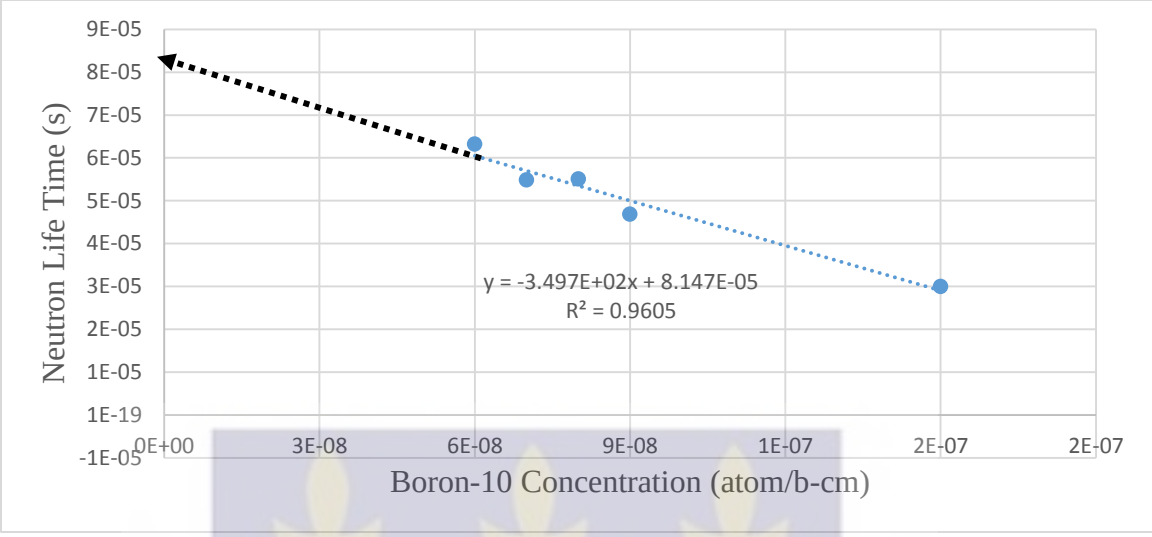

Figure.4.3 Plot of Neutron Life Time against Boron Concentration.

Table 4.2 Reactivity coefficients

Parameter	Temperature range (°C)	Irradiated core (mk/°C)	Clean Core (mk/°C)
Fuel Temperature Reactivity coefficient	20-40	-0.00347	
	50-100	-0.00294	
	200-600	-0.00266	-
Average(mk/°C)		-0.00303	-
Moderator void Reactivity coefficient	20-40	-0.08644	
	50-100	-0.19194	
Average (mk/°C)		-0.13871	-
Moderator Temperature (only) Reactivity Coefficient	20-40	0.007848	
	50-100	0.003924	
Average (mk/°C)		0.005886	
Combined Moderator Reactivity coefficient	20-40	-0.08921	
	50-100	-0.15456	
Average(mk/°C)		-0.12188	-0.13 (SAR)

4.1.1 Fuel Temperature Coefficient

The temperature reactivity coefficient was evaluated for the range 20°C to 600°C.This range was chosen as itincludes normal operating conditions and possible accident conditions. Figure 4.4 shows the relationship between reactivity and fuel temperature. The relationship between fuel temperature and reactivity is not linear. This is attributed to resonance behaviour of the fuel temperature cross section. The figure shows a regression of 0.416 which indicated a weak fit between data points. The correlation between the data was predicted to be -0.49062 which is a negatively weak. The reactivity coefficient was determined using the 3rd order differential equation and it is express by Equation 4.1

$$\alpha_T = -4.5\times10^{-13}T^4 + 4\times10^{-10}T^3 - 2.4\times10^{-7}T^2 + 4\times10^{-5}T - 0.0019 \qquad 4.1$$

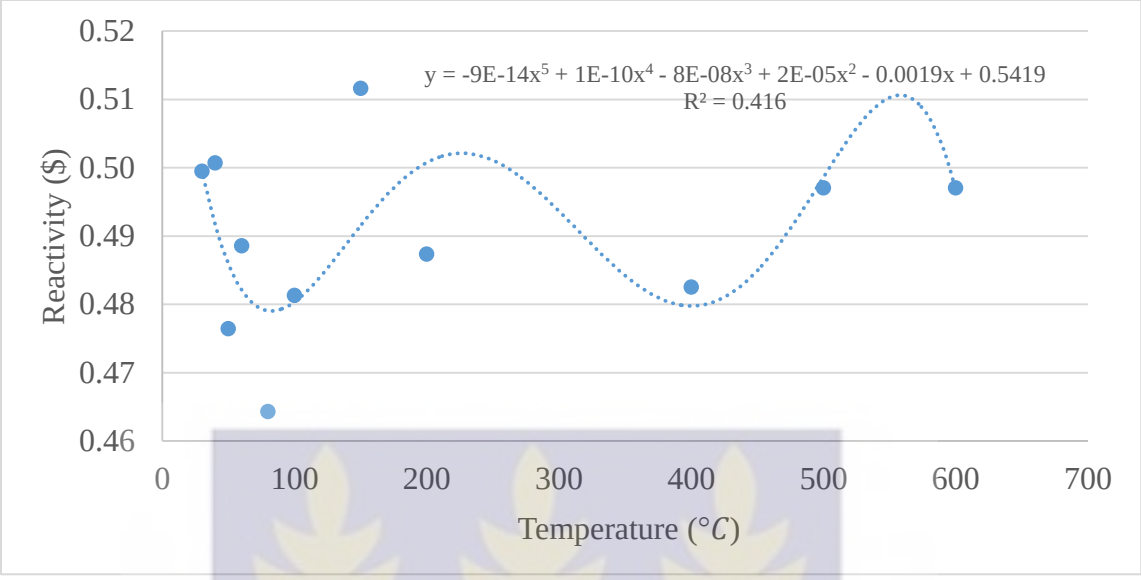

Figure.4.4. Fuel reactivity change with temperature.

4.1.2 Moderator Reactivity Coefficient

Figure 4.5 shows a relationship between reactivity changes due to moderator equilibrium temperature (MeV) with temperature (°C). The reactivity response to change in temperature is linear and as such it was determined using the 2nd order differential equation. The reactivity coefficient is given by Equation 4.2.

$$\alpha_M = -8\times10^{-6}T + 0.0012 \qquad 4.2$$

The graph shows a regression of 0.9811 which is fairly close to unit thus showing a good fit for the data. The correlation for the two parameters was determined to be 0.9822. This shows a strong positive correlation between reactivity and temperature. This implies, an increase in moderator equilibrium temperature (MeV) causes a corresponding increase in moderator temperature(°C).

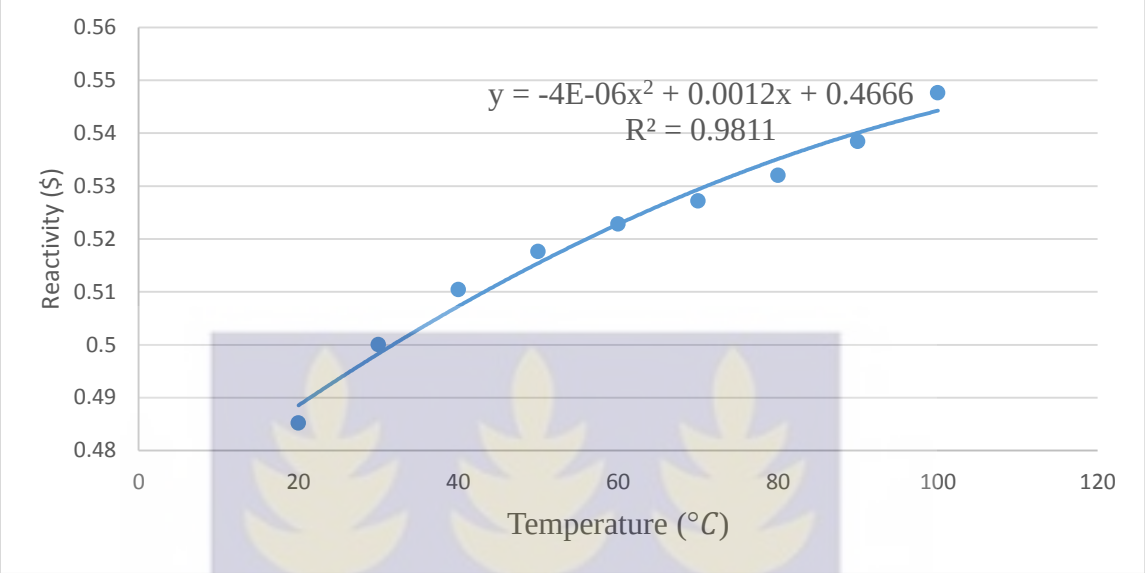

Figure 4.5. Moderator Temperature (MeV) change with temperature (°C)

Figure 4.6 shows the combined moderator equilibrium-temperature and void relationship with change in temperature. The response shows a strong negative correlation of -0.98777 which implies, an increase in moderator temperature causes a corresponding decrease in moderator density. A decrease in moderator density causes a decrease in the hydrogen atomic density and as such moderation is reduced. A reduction in moderation reduces the reactivity of the reactor as less neutrons cause fission. It can be concluded from Table 4.2 and Figure 4.6 that the temperature feedback becomes more negative for greater temperatures of water. Thus the reactor will not have any detrimental effects in case of any abnormal operations resulting in temperature increase.

$$\alpha_M = 9\times10^{-8}T^2 - 0.0002T - 0.005 \qquad 4.3$$

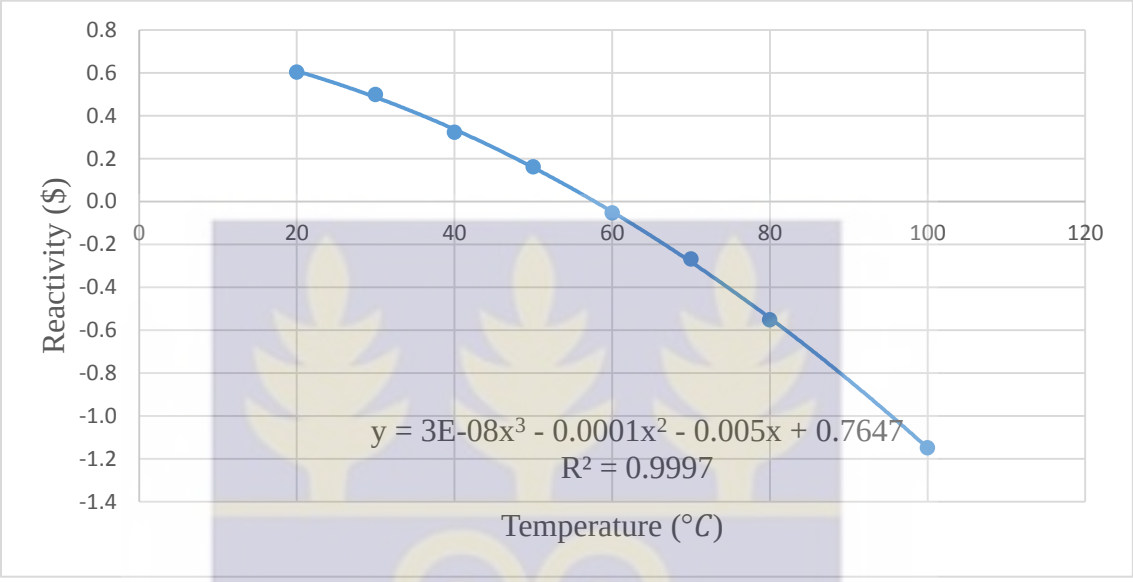

Figure 4.6. Combined Moderator void and Temperature (MeV) change with temperature (°C)

4.1.3 Moderator Void Coefficient

The moderator void coefficient (MVC) was predicted for the temperature range 20 °C to 100 °C. This was done to cover the normal operational range of the reactor. During normal operation of the reactor, the coolant temperature does not change significantly, however higher temperatures were chosen to study the behaviour of the moderator void coefficient at higher temperature.

The overall MVC for the temperature range described above was predicted to be negative. This is a safety feature of the MNSR. In case boiling occurs, the reactivity reduces thus preventing power excursion. Figure 4.7 shows the relationship of reactivity with density/void. The graph is best represented in terms of change with temperature. Where the temperature used corresponds to a specific moderator density, which in turn also corresponds to a specific void. The fit between the parameters was computed to be 0.9997 and the correlation was determined to be negatively strong as -0.9839. This entails, as temperature and voiding increases, reactivity will correspondingly reduce. This is also an MNSR safety feature which renders the reactor safe in case of an accidental insertion of reactivity which causes formation of voids or boiling. The void coefficient is given by Equation 4.4

$$\alpha_v = 3.0\times10^{-10}T^4 - 4\times10^{-8}T^3 + 1.8\times10^{-5}T^2 - 0.0016T + 0.021643 \qquad 4.4$$

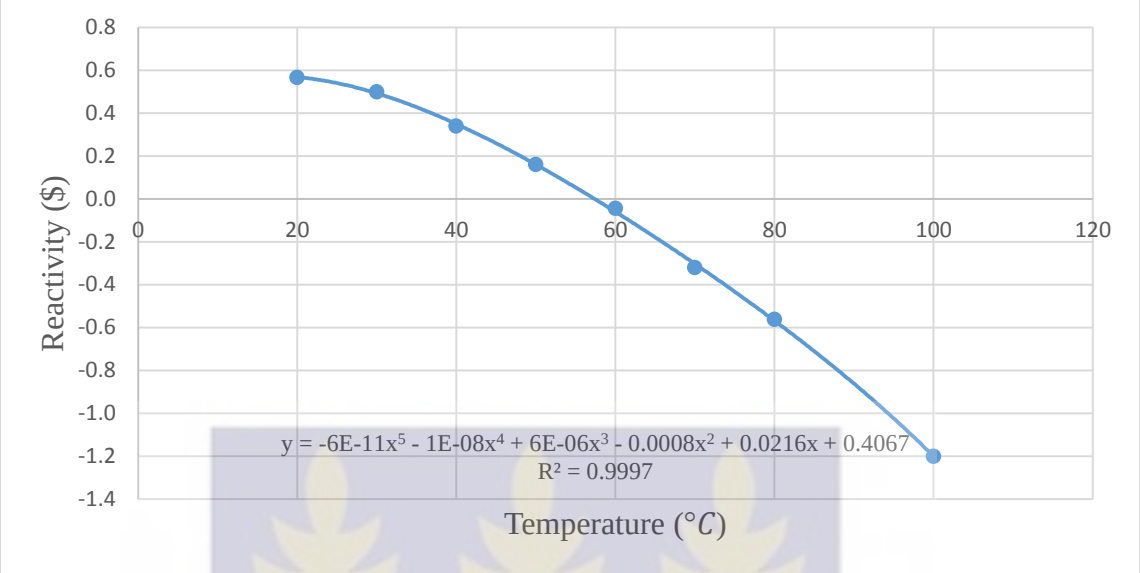

Figure 4.7. Moderator density (void) change with temperature (°C)

4.2 Thermal Hydraulics Parameters

4.2.1 Slow Transient Analysis

Table 4.3 compares feedback effects predicted in this work and those provided in [25], for reactivity insertion of 2.1 mk, 3.0 mk, 4.0 mk, 5.0 mk and 6.71 mk respectively. The results predicted from this work compare favorably with experimental data and that obtained from similar works. However, PARET/ANL code was not able to simulate correctly reactivity insertions for 5.0 mk and 6.71 mk. This is graphically evident through the spikes that are observed in Figures4.10 and 4.11.These spikes could be attributed to PARET/ANL's failure to switch between thermal-hydraulic flow regimes[14,23].

Table 4.3 Comparison of reactivity feedback between this work and experimental data

Reactivity Insertion (mk)	Maximum Power (kW)		Fuel Temperature (°C)		Clad surface temperature (°C)		Coolant outlet temperature (°C)	
	Exp.	This work	Exp.	This work	Exp.	This work	Exp.	This work
2.1	36.1	39.3	66.3	64.1	-	63.5	47.0	51.6
3.0	-	55.3	83.0	74.2	82.5	73.3	57.7	57.8
4.0	100.2	91.2	-	93.6	-	92.2	-	69.6
5.0	60.9	130	-	111	-	109	58.4	79.9
6.71	-	202	-	137	-	134	-	96.3

The results presented in table 4.3 are plotted in Figures 4.8 to 4.11. It is observed from Figure 4.11 that for higher reactivity insertion the power rises sharply within seconds of reactivity insertion. However, for lower reactivity insertions the rise in power is gradual. The 6.71 mk reactivity insertion has a quick rise in power but attains its maximum power in 600 s. The 2.1 mk and 3.0 mk have a slow rise in power but attain their maximum power in 612 s and 606 s respectively. For reactivity insertions 4.0 mk and 5.0 mk, the maximum power was attained at 144.36 s and 144.06 s respectively.

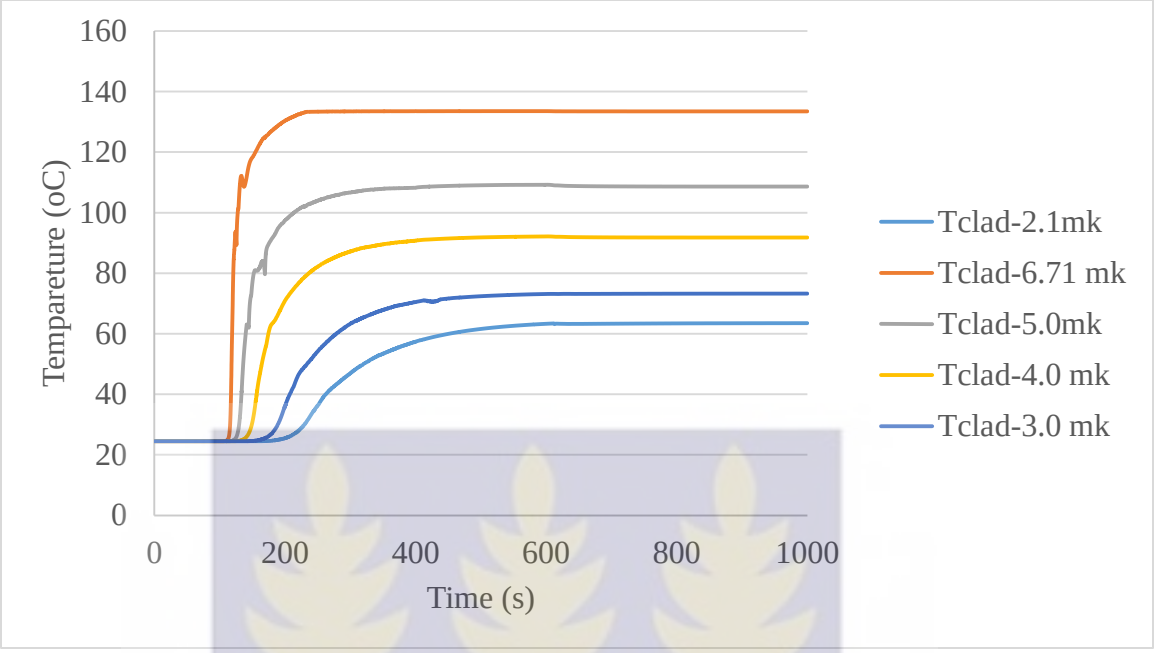

Figure 4.8 Plot of Clad temperature for 2.1 mk, 4.0 mk, 5.0 mk and 6.71 mk reactivity insertion

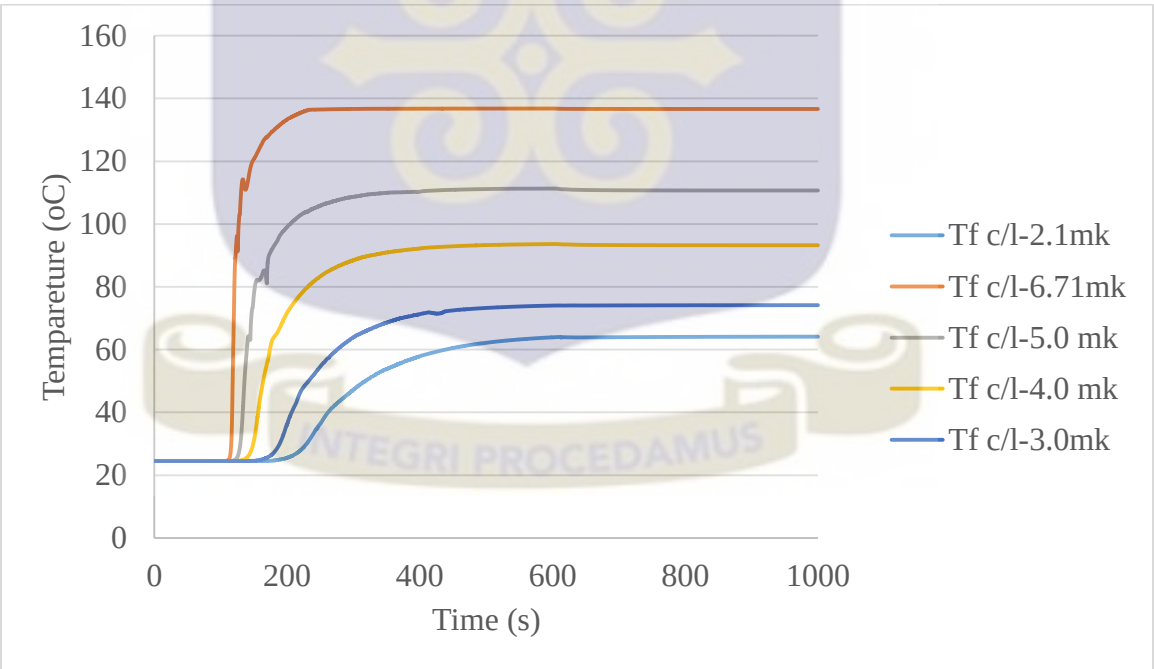

Figure 4.9 Plot of Fuel center line temperature for 2.1 mk, 4.0 mk, 5.0 mk and 6.71 mk reactivity insertion.

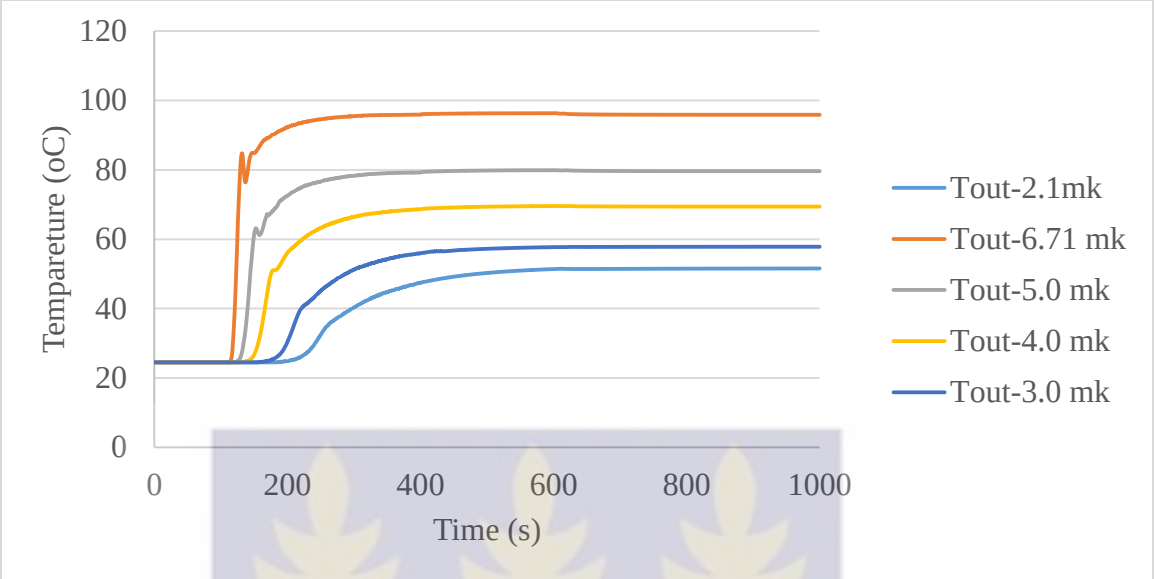

Figure 4.10 Coolant outlet temperatures for 2.1 mk, 3.0 mk, 4.0 mk, 5.0 mk and 6.71 mk reactivity insertion.

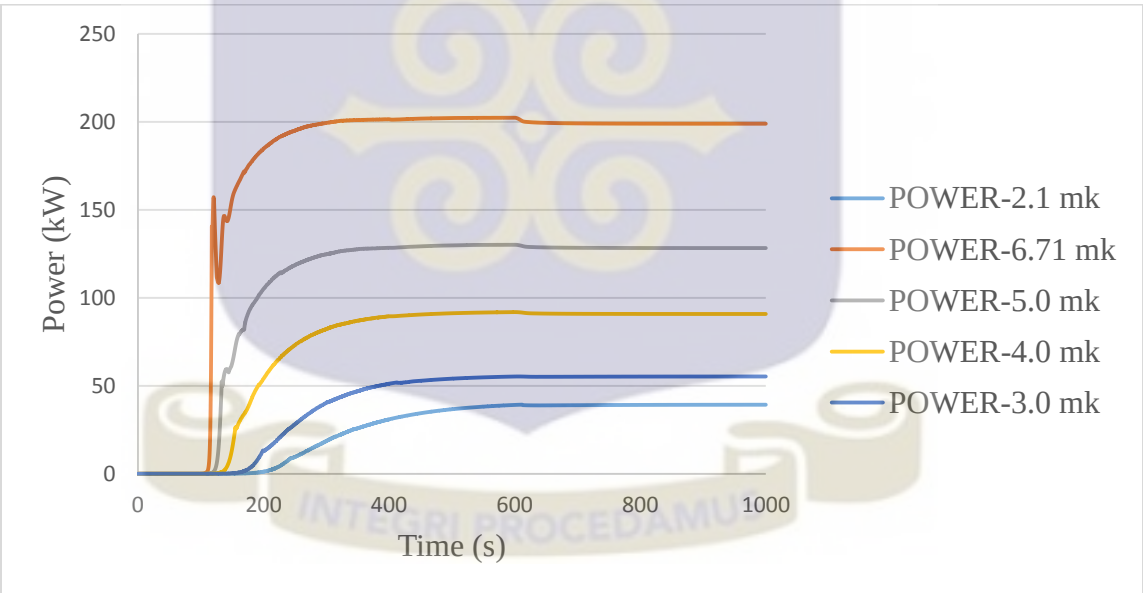

Figure 4.11Plot of reactor power for 2.1 mk, 3.0 mk, 4.0 mk, 5.0 mk and 6.71 mk reactivity insertion.

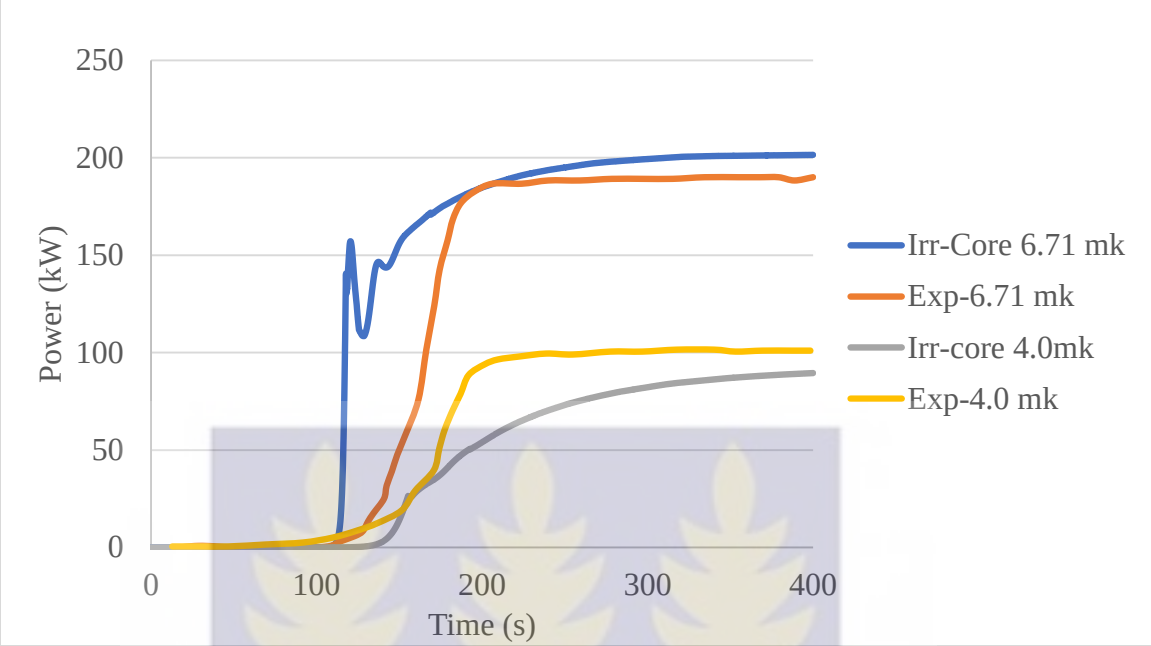

Figure 4.12Comparison of Reactor Power (kW) for 4.0 mk and 6.71 mk Reactivity Insertion and Experimental Work (Akaho and Maakuu, 2002)

4.2.2 Fast Transients Analysis

Figures 4.13 and 4.14 show the feedback effect due to a postulated accident in which the excess reactivity of 3.86 mk was inserted into the core. During the transient, the reactor power increases to a maximum value of 87 kW in 600 s which is 2.9 greater than the nominal power. This value is above the allowed limit of 120%of the nominal power.

The maximum fuel centerline, clad surface and coolant outlet temperatures were predicted to be 92.3°C, 90.1 °C and 68 °C respectively. The clad and fuel temperatures are below the 640 °C melting point of the U-Al alloy. The coolant outlet temperature was predicted to be slightly above the 120% of the nominal temperature limit.

Despite these values being greater than the 120% limit, boiling would not occur as the coolant outlet temperature is below the 113 °C saturation temperature provided in [25, 43] and the115.18 °C predicted in this work and the 117.1 °C ONB temperature.

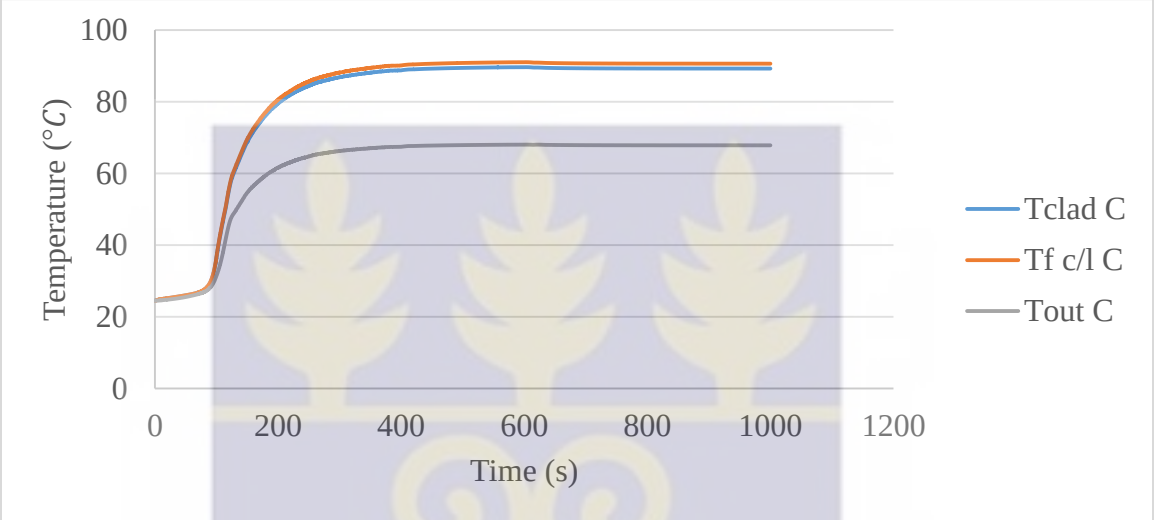

Figure 4.13 Plot of fuel centerline, clad and coolant outlet temperatures for fast reactivity insertion 3.86 mk/0.5s

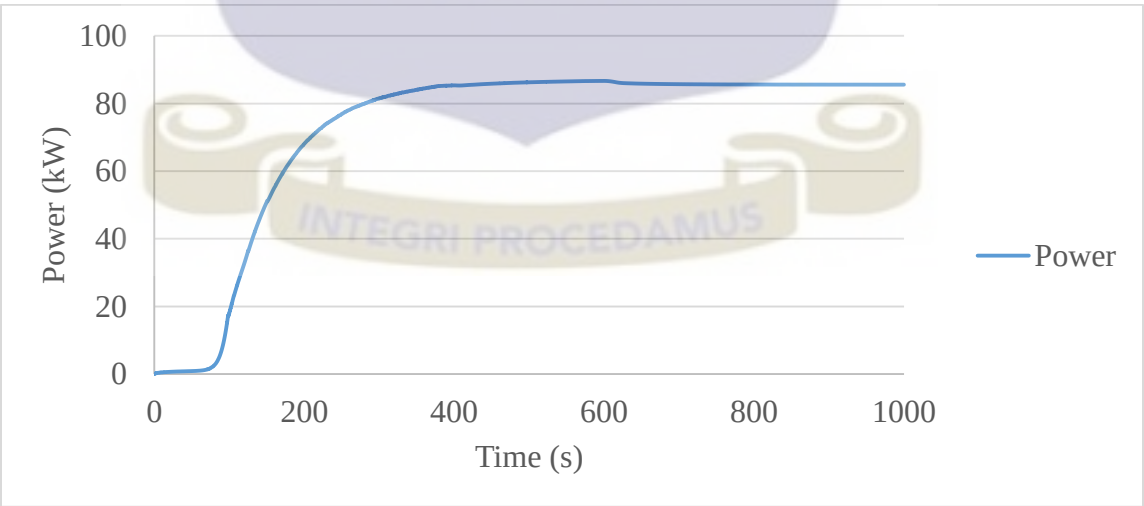

Figure4.14Plot of Power against time for design basis accident.

4.2.3 Steady State Analysis

Table 4.4 Comparison of Steady State Parameters predicted by PARET/ANL and PLTEM/ANL Codes

PARAMETER	PARET/ANL		PLTEMP/ANL		Safety Analysis Report (SAR)	
	15 kW	30 kW	15 kW	30 kW	15 kW	30 kW
Coolant Inlet temperature (°C)	24.5	24.5	24.5	24.5	24.5	24.5
Coolant outlet temperature (°C)	41.67	51.1	37.9	44.6	-	44.5
Coolant temperature rise (°C)	17.17	26.6	13.4	20.1	13.0	20.0
Maximum Clad temperature (°C)	47.5	60.8	72.1	99.1	71.6	99.8
Maximum Fuel temperature (°C)	47.78	61.28	-	-	71.8	100.1

The results obtained for the steady state thermal hydraulics parameters for both the 15 kW and the 30 kW models compare favorably with those in literature. Table 4.4compares the steady state parameters obtained by PLTEMP/ANL code, PARET/ANL code, and those provided in literature and [25]for power ratings of 15 kW and 30 kW respectively. It is observed from the table that the PLTEMP/ANL code was able to correctly predict most of the parameters compared to PARET/ANL code. This can be attributed to the differences in the correlations used in predicting the flow regimes. The PARET/ANL code requires an input of more of neutronics parameters compared to PLTEMP/ANL

code. This implies PARET/ANL model carries over more uncertainties compared PLTEMP/ANL model.

The coolant temperature rise was well predicted by PLTEMP/ANL with a difference of 0.375°C compared to the difference of 4.17 °C by PARET/ANL. This indicates that the PLTEMP/ANL model was quite representative of GHARR-1 after 19 years of operation and that the power peaking factors that were obtained from the MCNP simulation were also representative of the core.

The PARET/ANL code has no capacity to predict ONBR, DNBR and FIR. These were only predicted by PLTEMP/ANL and the results indicate a good agreement with the values obtained during the calibration of PLTEM/ANL code for use in research reactors with solid fuel rods for calculating natural circulation.

The minimum flow instability power ratio (FIR) or the Onset of Flow instability (OFI) for both the 15 kW and 30 kW power rating were predicted as presented in Table 4.5 and indicate a good agreement with those provided in [43]. Using the simplified Babelli-Ishii criterion, described by Equation 2.39, the coolant flow is stable as the Subcooling Number/Zuber Number ratio was predicted to be above the 1.36. The minimum value for the Subcooling Number/Zuber Number ratio was predicted to be 1306.7 greater than 1.0007 on the RHS of criterion for channel 1 and 5.601 greater than 1.0673 on the RHS of criterion for channel 2.

The DNBR for 15 kW and 30 kW power rating for the outer surface of the clad were predicted to be greater than the minimum 2.5 thermal hydraulic design criteria for the MNSRs [25]. Figure 4.15 shows the DNBR for the inner surface as a function of distance along the hot rod. For both 15 kW and 30 kW models, the DNBR occurs on the 11^{th} node which is 0.1265 m from the bottom of the fuel meat.

Table 4.5 Comparison of Steady State Safety Parameter Margins

PARAMETER	**PLTEMP/ANL**		**Safety Analysis Report [25]*/Reference [43]****	
	15 kW	**30 kW**	**15 kW**	**30 kW**
Burnout Ratio (DNBR) Outer	36.1	19.12	-	21.7**
Inner	2.29	1.48	-	-
Onset of Nucleate Boiling Ratio (ONBR)	1.94	1.25	-	1.23**
Flow Instability Power Ratio (FIR)	6.57	4.37	-	4.4**
Onset of nucleate boiling temperature (°C)	116.79	117.1	-	116.9**
Saturation Temperature (°C)	115.18	115.18	113*	113**
CHF Temperature	-	162.15	-	-

Note * Result compared with that provided in reference [25]

**Result compared with that provided in reference [43]

The critical burnout flux (which is the limiting flux) for 30 kW power rating for the outer and inner surface of the clad were predicted to be 0.477 MW/m^2 and 0.044 MW/m^2 with

the operating flux predicted as 0.0248 MW/m^2 and 0.0297 MW/m^2 respectively. The actual operating flux for the outer surface was hand calculated as 0.02194 MW/m^2 using Equation 2.32.

The critical heat flux for the 15 kW power rating for the outer and inner surface of the clad were predicted to be 0.468 MW/m^2 and 0.0355 MW/m^2 with the operating flux predicted as 0.0125 MW/m^2 and 0.0155 MW/m^2 respectively. The actual operating flux for the outer surface was hand calculated as0.010972 MW/m^2.

The ratios for the critical burnout flux to the actual operating flux gave the DNBR presented in Table 4.4. The DNBR sets an operational margin that puts a limit to operating conditions that would otherwise compromise the integrity of the clad [35].

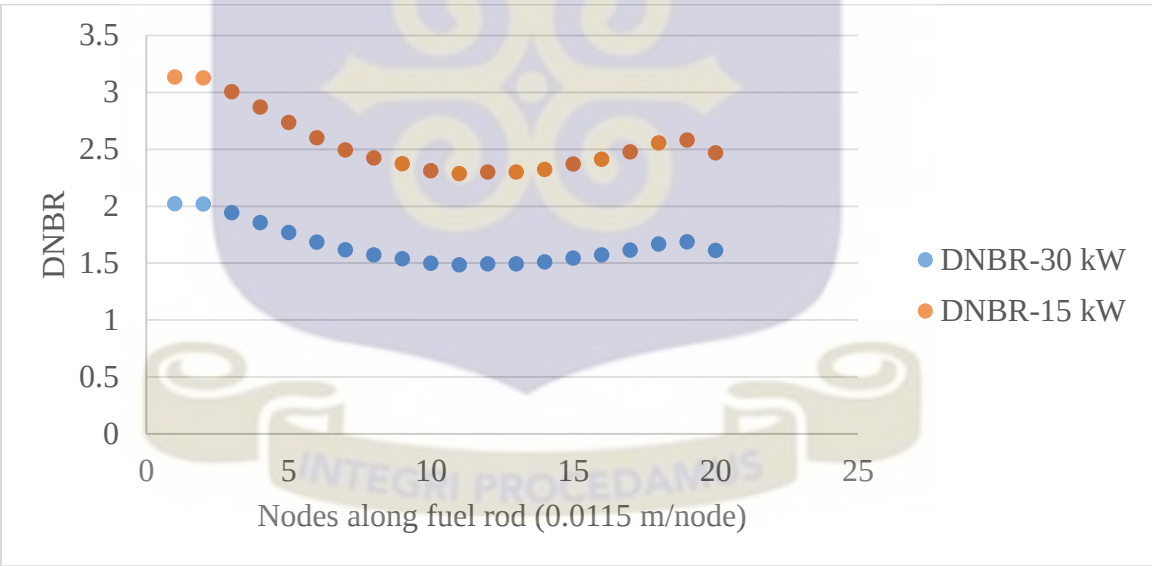

Figure 4.15Departure from nucleate boiling ratio for the inner surface as a function of position along the hot-rod fuel element

The ONBR as described by Equation 2.29 which is given as a ratio of the difference between the ONB temperature and the coolant inlet temperature, and the difference between the clad surface temperature and the coolant inlet temperature.

The limiting value for the ONBR for 30 kW power rating was computed as 92.8 °C and the maximum clad surface and coolant inlet temperature difference as 74.56 °C. The ONB temperature was predicted as 117.3°C.

The limiting temperature difference for the 15 kW power rating was computed as 92.29 °C with the ONB temperature predicted as 116.79. The limiting maximum operating temperature difference between the clad surface and coolant inlet temperatures was computed as 47.63°C.

From Equation 2.29, the parameter that is changing is clad surface temperature. An increase in the clad surface temperature implies a reduction in the ONBR. Thus, an increase in clad surface temperature above the saturation temperature would cause nucleation.

The predicted surface temperatures for both 15 kW and 30 kW indicated that boiling would not occur in the channels. This is as a result of the surface temperature being far below the predicted ONB temperature for both power ratings.

CHAPTER FIVE

CONCLUSION AND RECOMMENDATIONS

The safe operation of a nuclear reactor is enhanced by having periodical evaluation of safety parameters. Besides the periodical evaluation, each time changes are made to the core, safety parameters should be evaluated. Safety parameters for GHARR-1 after 19 years of operation have been evaluated. The neutronics and thermal hydraulics were coupled using PARET/ANL and PLTEMP/ANL codes.

The neutronic parameters that were used in coupling with thermal hydraulics were predicted using MCNP5 code. These parameters are; neutron generation time, delayed neutron fraction, reactivity coefficients, axial and radial power peaking factors. The axial and radial power peaking factors were used in PLTEMP/ANL to predict the ONBR, DNDR, and OFI. The other neutronic parameters, in exception of the radial power peaking factors were used in the PARET/ANL code for analysis of both steady state, transients (slow and fast). The results obtained for both neutronics and thermal hydraulics are in good agreement with those provided in [25] and elsewhere in literature. In some cases data was generated that could be included in the [25].

The results obtained suggests GHARR-1 is safe to be operated with a reactivity insertion of 2.1 mk as the clad surface and the coolant outlet temperatures obtained would not support boiling to occur in the cooling channel. Besides this, the results obtained for the 2.1 mk are well below the limit set for which the reactor power and coolant outlet should not exceed 120% of the nominal operating parameter. However, for reactivity insertions covering the range 2.1 mk to 6.71 mk, no boiling can occur in the cooling channel.

The results obtained satisfy the design criteria for safety analysis of the reactor and the trend in results is comparable to that documented in the IAEA-TECDOC-643 [10].

RECOMMENDATIONS

More work needs to be done on the observed overlap in the power distribution for the irradiated core and the clean core presented in Figure 4.1 and 4.2.

With respect to fuel depletion and buildup of fission products, neutronic calculations to predict the 6 group and 15 groups of delayed neutron fractions can be done to see if there are any major changes.

A code could be developed that could link the four codes that were used in this work as a way of improving on the accuracy of the data generated.

The effect of spectrum softening, due to buildup of fission products, on neutron generation time should be investigated on the core of GHARR-1.

The results obtained in this work can be used as a basis for similar works to be carried out in future and it can also be used as a source of comparison.

REFERENCES

[1] Borio A., Bradley E., Ridikas D., Vyshniauskas J., Research Reactors Coalitions, [Online] Available: http://www.iaea.org/NuclearPower/Downloadable/Meetings/2013/2013-11-27-11-28-TM-INIG/2-Borio_IAEA_TM_Networking.pdf. [September 30, 2014].

[2] IAEA Brochure. Research Reactors in Africa. [Online] Available: http://www.iaea.org/OurWork/NE/NEFW/Technical Areas/RRS/documents/RR_in_Africa.pdf. [30th September 2014]

[3] ANL Reactor Homepage website, Argonne National Laboratory, http://www.anl.gov/

[4] Woodruff, W.L., (1982). The PARET/ANL Code and the Analysis of the SPERT I Transients, ANL/RERTR/TM – 4.

[5] Zafar, U.K, (2006). An elementary model to study sensitivity of the Departure from Nucleate Boiling Ratio (DNBR) to perturbations in nuclear reactor systems. ARPN Journal of Engineering and Applied Sciences 1 (1), ISSN 1819-6608.

[6] Ravink, M.,(2000). Report on nuclear data and nuclear reactors workshop, Physics design and safety, Trieste,13th March-14 April 2000.

[7] Keng, Y.C., (2009). Thermal-Hydraulics limits for MIT Research Reactor Low Enriched Uranium core conversion using statistical propagation of parametric uncertainties, National Tsing-Hua University, Taiwan.

[8] Akaho, E.H.K., (2014). Reactor thermal-hydraulics lecture notes, NSTP-638, University of Ghana School of Nuclear and Allied Sciences, Nuclear Engineering Department, Accra, Ghana, 2013-2014.

[9] Cardoni J.N. Nuclear reactor multi-physics simulations with coupled MCNP5 and STAR-CCM+.International Conference on Mathematics and Computational Methods Applied to Nuclear Science and Engineering (M&C 2011) Rio de Janeiro, RJ, Brazil, May 8-12, 2011.

[10] IAEA-TECDOC-643, (1992). Research Reactor Core Conversion, Analytical Verification Guidebook - Volume 3.

[11] Cardoni, J.N, Nuclear reactor multi-physics simulations with coupled MCNP5 and STAR-CCM+.International Conference on Mathematics and Computational Methods Applied to Nuclear Science and Engineering (M&C 2011) May 8-12, 2011, Rio de Janeiro, RJ, Brazil.

[12] X-5 Monte Carlo Team, (2008).MCNP – A General Monte Carlo N-Particle Transport Code, Version 5, Los Alamos, New Mexico

[13] Ampomah-Amoako, E., Akaho, E.H.K., Anim-sampong, S., Nyarko, B.J.B., (2009). Transient analysis of Ghana Research Reactor-1 using PARET/ANL thermal hydraulic code, Nuclear Engineering and Design 234.

[14] Akaho, E.H.K., Anim-Sampong, S., Maakuu, B.T., Dadoo-Amoo, D.N.A., (2000). Dynamic feedback characteristics of Ghana research reactor-1. Journal of the Ghana Science Association 2 (3), 200–208.

[15] Olson, A.P., Jonah, S.A., (2007).MNSR transient analyses and thermal–hydraulic safety margins for HEU and LEU cores using PARET/ANL code. In: RERTR-2007 International Meeting on Reduced Enrichment for Research and Test Reactors, Prague, Czech Republic, 23–27 September.

[16] Anim-Sampong, S., (2001). Three-dimensional monte carlo modeling and particle transport simulation of the Ghana Research Reactor-1, technical report, NNRI/GAEC/ICTP/ENEA-TR.01/2001.

[17] Adooa, N.A, Nyarkoa, B.J.B., Akahoa, E.H.K., Alhassana, E., Agbodemegbea, V.Y., Bansaha, C.Y., Dellaa. R., (2011). Determination of thermal hydraulic data of GHARR-1 under reactivity insertion transients using the PARET/ANL code.

[18] Boafo, E.K., (2012). Assessing the Effect of Fuel Burnup on Control Rod Worth for HEU and LEU Cores of GHARR-1, Research Journal of Applied Sciences, Engineering and Technology 5(4): 1129-1133, 2013 ISSN: 2040-7459; e-ISSN: 2040-7467

[19] Ahmed, Y.A., Balogun, G.I., Jonah, S.A., Funtua, I.I., (2008). The behaviour of reactor power and flux resulting from changes in core-coolant temperature for a miniature neutron source reactor. Annals of Nuclear Energy 35, 2417–2419.

[20] Hainoun, A., Alisa, S., (2005). Full-scale modeling of the MNSR reactor to simulate normal operation, transients and reactivity insertion accidents under natural circulation conditions using the thermal hydraulic code ATHLET. Nuclear Engineering and Design 235, 33–52.

[21] Jonah, S.A., Liaw, J.R., Matos, J.E., (2007). Monte Carlo simulation of core physics parameters of the Nigeria research reactor-1 (NIRR-1). Annals of Nuclear Energy 34, 953–957.

[22] Alhassan, E.,(2010). Analysis of Reactivity Temperature Coefficient for Light Water Moderated HEU-UAl4 and LEU-UO2 Lattices of MNSR, Journal of Applied Sciences Research, 6(9): 1431-1439, INSInet Publication.

[23] Daniel, J. S., 2013. A Safety Analysis of an Accidental Reactivity Excursion in the University of Florida Training Reactor.

[24] Bretscher, M. M., Hanan, N. A., Matos J. E., Neutronic Safety Parameters and Transient Analyses for Poland's Maria Research Reactor. Paper presented at the International Meeting on Reduced Enrichment for Research and Test Reactors, 3-8 October, 1999, Budapest, Hungary.

[25] Akaho, E.H.K., Anim-Sampong, S.,Dodoo- Amoo, D.N.A., Maakuu, B.T., Emi Reynolds, G., Osae, E.K., Boadu, H.O., Bamford, S.A., (2003). Ghana Research Reactor-1 Final Safety Analysis Report. Ghana Atomic Energy Technical Report, GAEC-NNRIRT-90.

[26] Anim-Sampong, S., Akaho, E.H.K., Boadu, H.O., Intsiful, J.D.K., Osae, S., (1999). Fuel Depletion Analysis for the HEU core of GHARRR-1; Part I; Actinide Inventory. A Paper Presented at a Meeting on Reduced Enrichment for Research and Test Reactors, Budapest, Hungary, October 3–8, 1999.

[27] Anim-Sampong, S., Akaho, E.H.K., Maakuu, B.T., Gbagbo, J.K.,Andam, A., Liaw, J.J.R., and Matos, J.E., (2007). Neutronics Analysis for Conversion of the Ghana Research Reactor-1 Facility using Monte Carlo Methods and UO2 LEU Fuel. In proceeding of the IRRFM 2007/IGORR, Session VI - Safety, Operation and Research Reactor Conversion, pp: 44-54.

[28] Yue-wen, Y., (1993). Reactor Complex; an MNSR Training Material. CIAE Technical Report, Beijing,China.

[29] Zafar, U.K., (2006). An elementary model to study sensitivity of the Departure from Nucleate Boiling Ratio (DNBR) to perturbations in nuclear reactor systems. ARPN Journal of Engineering and Applied Sciences 1 (1), ISSN 1819-6608.

[30] IAEA-TECDOC-643, 1992. Research Reactor Core Conversion, Analytical Verification Guidebook - Volume 3.

[31] Cardoni, J.N., Nuclear reactor multi-physics simulations with coupled MCNP5 and STAR-CCM+.International Conference on Mathematics and Computational Methods Applied to Nuclear Science and Engineering (M&C 2011) Rio de Janeiro, RJ, Brazil, May 8-12, 2011.

[32] X-5 Monte Carlo Team, "MCNP – A General Monte Carlo N-Particle Transport Code, Version 5," Los Alamos, New Mexico (2008).

[33] Adoo, N.A, Nyarko, B.J.B., Akaho, E.H.K., Alhassan, E., Agbodemegbe, V.Y., Bansah, C.Y., Della. R., (2011). Determination of thermal hydraulic data of GHARR-1 under reactivity insertion transients using the PARET/ANL code.

[34] Henryk, A.,(2005). Lectures on Applied Reactor Technology and Nuclear Power Safety, Nuclear Reactor Technology Division, Department of Energy Technology, KTH. Lecture 03.

[35] Lamarsh, J. R., Anthony J. Baratta; Introduction to Nuclear Engineering, third edition, 2001. Prentice-Hall Inc.

[36] Ampomah-Amoako, E., (2013-2014). Reactor Kinetics lecture notes. NSTP648, SNAS–Nuclear Engineering, University of Ghana.

[37] Jacopo, B, Notes on Two-Phase flow Boiling Heat Transfer and Boiling Crises in PWRs and BWRs, MIT Department of Nuclear Science and Engineering 22.06 Engineering of Nuclear systems 2010.

[38] http://www.mne.psu.edu/me315/Boiling.pdf

[39] Olson, A. P., Kalimullah. (2010). A User's Guide to the PLTEMP/ANL V4.0 code. Global Threat Reduction Initiative (GTRI) Argonne National Laboratory.

[40] Olson, A. P., (2001). A User's Guide to the REBURS-PC code V 1.4. Argonne National Laboratory.

[41] BRETSCHER, M. M. Evaluation of Reactor Kinetic Parameters without the Need for Perturbation Codes, Proc. Int. Meeting on Reduced Enrichment for Research and Test Reactors, Oct.1997, Wyoming, USA.

[42] Woodruff, W. L (2002). A Users Guide for the Current ANL Version of the PARET/ANL Code, Argonne National Laboratory, Distributed by the Radiation Shielding Information Computational Center (RSICC) at Oak Ridge National Laboratory as Software Package PSR-516, Feb. 2002

[43] Kalimullah M., Olson A.P., (2010). Testing the PLTEMP/ANL Code for Calculating Natural Circulation in a Research Reactor Having Solid Fuel rods, Argonne National Laboratory.

[44] Hanson A. L and Diamond D. J., (2012). Calculation of Kinetics Parameters for the NBSRNuclear Science and Technology Department Brookhaven National Laboratory.

APPENDICES

APPENDIX A

ISOTOPIC DENSITIES FOR THE IRRADIATED CORE USED TO UPDATE THE MATERIAL CARD IN MCNP INPUT DECK

	MCNP LIBRARY	MASS	ISOTOPE	
1	92235.66c	2.46E-01	U-235	
2	92238.66c	2.78E-02	U-238	
3	92234.66c	7.97E-10	U-234	
4	92236.66c	3.10E-06	U-236	
5	53135.50c	3.24E-07		
6	54135.50c	1.92E-07		
7	61149.50c	1.01E-07	Pm-149	
8	62149.50c	8.09E-09	Sm-149	
9	93237.50c	1.12E-10	Np-237	
10	94238.50c	5.37E-16	Pu-238	
11	94239.50c	1.08E-07	Pu-239	
12	94240.50c	7.98E-13	Pu-240	
13	94241.50c	1.34E-17	Pu-241	
14	94242.50c	4.29E-23	Pu-242	
15	95241.50c	2.21E-22	Am-241	
16	61147.70c	1.43E-06	Pm-147	LUMP
17	61148.70c	1.31E-13	Pm-148	LUMP

18	61548.70c	1.29E-12	Pm-148m	LUMP
19	55137.70c	8.93E-09	Cs-137	LUMP
20	48113.70c	4.18E-07	Cd-113	LUMP
21	55133.70c	2.75E-06	Cs-133	LUMP
22	54131.70c	3.49E-06	Xe-131	LUMP
23	45103.70c	3.18E-13	Rh-103	LUMP
24	36085.70c	3.38E-12	Kr-85	DUMP
25	56140.70c	3.26E-12	Ba-140	DUMP
26	58141.70c	5.91E-11	Ce-141	DUMP
27	38089.70c	8.55E-13	Sr-89	DUMP
28	38090.70c	1.83E-12	Sr-90	DUMP
29	93236.70c	5.09E-09	Np-236	DUMP
30	93238.70c	4.25E-09	Np-238	DUMP
31	13027.92c	7.21E-01	Al Matrix	
32	5010.66c	5.15E-07	*Boron-10 18.4%	
33	5011.66c	2.28E-06	*Boron-11 81.6%	
34	24000.50c	2.40E-04	Chromium	
35	6012.50c	6.50E-04	Carbon	
36	48000.50c	1.00E-06	Cadmium	
37	3006.66c	1.04E-06	* Lithium as m7	
38	3007.66c	1.50E-05	* Lithium as m7	
39	26000.55c	7.25E-04	Iron	
40	28000.50c	4.50E-04	Nickel	
41	4009.66c	5.00E-08	beryllium	
42	7014.62c	2.00E-05	* Nitrogen	

43	12000.62c	1.00E-05	*Magnesuim	
44	20000.62c	2.00E-05	Calcium	
45	64000.35c	2.50E-07	Gadolinium	

APPENDIX B

SAMPLE INPUT DECK FOR MCNP

```
c  HEU 344-Pin for GHARR-1 - 28/11/2014 with 10.9 cm of beryllium added
c
c ********************
c SECTION 1: CELL DATA
c ********************
c
c            FUEL CAGE AND LATTICE ASSEMBLY
c
c          CONTROL ROD AND GUIDE TUBE CELLS
c
c          COMPLETE WITHDRAWAL OF CONTROL ROD
c
1 3 -0.99567 -1 -3 4          imp:n=1 tmp=2.6124e-08 $ Cd control rod or water
2 3 -0.99567  1 -2 -3 4       imp:n=1 tmp=2.6124e-08 $ SS-304 clad or water
3 3 -0.99567  2 -5 -3 4       imp:n=1 tmp=2.6124e-08 $ Water in guide tube
4 4 -2.70000  5 -6 -3 4       imp:n=1 tmp=2.5262e-08 $ Guide tube material,
c
c                PARTIAL INSERTION
c
```

c 1 1 -8.65000 -1 -3 84 imp:n=1 tmp=2.5262e-08 $ Cd control rod or water (3 -1.00000)

c 2 2 -7.80000 (1 -2 -3 84) &

c :(-2 82 -84) imp:n=1 tmp=2.5262e-08 $ SS-304 clad or water (3 -1.00000)

c 3 3 -0.99567 (-5 4 -82):(2 -5 82 -3) imp:n=1 tmp=2.6124e-08 $ Water in guide tube

c 4 4 -2.70000 5 -6 -3 4 imp:n=1 tmp=2.5262e-08 $ Guide tube material,

c

c

c ACTIVE ZONE CELLS OF FEUL ASSEMBLY

c

c meat ASSEMBLY FOR RADIAL DISTRIBUTION OF NEUTRONIC PARAMETERS

c

c A LL A TTTTT TTTTTT II CCCC EE EEE

c A A LL A A TT TT II CC EE

c AAAAA --- LL AAAAA TT TT II CC EE EEE

c AA AA --- LL AA AA TT TT II CC EE

c AAAA LLLLL AA AA TT TT II CCCC EE EEE

c

c FIRST RING OF 6 FUEL ELEMENTS

c

6 6 -3.45600 -11 -3 4 imp:n=1 tmp=3.4470e-08 $ meat 1 first density = 3.47617

```
7  13 -2.70000   11 -111 -3 4       imp:n=1 tmp=2.5262e-08 $ clad
8  6 -3.45600  -12 -3 4            imp:n=1 tmp=3.4470e-08 $ meat 2
9  13 -2.70000   12 -121 -3 4       imp:n=1 tmp=2.5262e-08 $ clad
10 6 -3.45600  -13 -3 4            imp:n=1 tmp=3.4470e-08 $ meat 3
11 13 -2.70000   13 -131 -3 4       imp:n=1 tmp=2.5262e-08 $ clad
12 6 -3.45600  -14 -3 4            imp:n=1 tmp=3.4470e-08 $ meat 4
13 13 -2.70000   14 -141 -3 4       imp:n=1 tmp=2.5262e-08 $ clad
14 6 -3.45600  -15 -3 4            imp:n=1 tmp=3.4470e-08 $ meat 5
15 13 -2.70000   15 -151 -3 4       imp:n=1 tmp=2.5262e-08 $ clad
16 6 -3.45600  -16 -3 4            imp:n=1 tmp=3.4470e-08 $ meat 6
17 13 -2.70000   16 -161 -3 4       imp:n=1 tmp=2.5262e-08 $ clad
.

..

.

.
m6   92235.66c -0.2464573            $ U-235 endf66c from ENDF/B_VI.5 (1997),
92235.50c
    92238.66c -0.0277806             $ U-238 ENDF66C FROM endf/b-vi.5 (1993),
92238.50c
    92234.66c -0.000000000797451     $ U-234 ENDF66C FROM endf/b-vi.5 (1993),
92234.50c added 6/9/09 - JRL
    92236.66c -0.00000310327         $ U-236
    53135.50c -0.000000324388            $ I-135
```

54135.50c -0.000000191569 $ Xe-135

61149.50c -0.000000100661 $ Pm-149

62149.50c -0.00000000808585 $ Sm-149

93237.50c -0.00000000011186 $ Np-237

94238.50c -5.37413E-16 $ Pu-238

94239.50c -0.000000107566 $ Pu-239

94240.50c -0.000000000000798061 $ Pu-240

94241.50c -1.34419E-17 $ Pu-241

94242.50c -4.28558E-23 $ Pu-242

95241.50c -2.21482E-22 $ Am-241

61147.70c -1.4341724E-06 $ Pm-147 LUMP

61148.70c -1.3065688E-13 $ Pm-148

61548.70c -1.2940532E-12 $ Pm-148m

55137.70c -8.9255674E-09 $ Cs-137

48113.70c -4.1819975E-07 $ Cd-113

55133.70c -2.7502849E-06 $ Cs-133

54131.70c -3.4872756E-06 $ Xe-131

45103.70c -3.1828674E-13 $ Rh-103

36085.70c -3.38050822E-12 $ Kr-85 DUMP

56140.70c -3.25832118E-12 $ Ba-140

58141.70c -5.90570714E-11 $ Ce-141

38089.70c -8.55309310E-13 $ Sr-89

38090.70c -1.83280566E-12 $ Sr-90

93236.70c -5.09112684E-09 $ Np-236

93238.70c -4.25210914E-09 $ Np-238

c 93239.70c -6.47183115E-11 $ Np-239

13027.92c -0.7214049 $ Al Matrix 0.7213998= wt% of Al in meat, 0.000010= wt % in alloy

5010.66c -0.0000005152 $ *Boron-10 18.4% ENDF66a from ENDF/B-VI.1 (5010.50c)

5011.66c -0.0000022848 $ *Boron-11 81.6% ENDF66a from ENDF/B-VI.1 (5010.50c)

24000.50c -0.0002400 $ Chromium

6012.50c -0.0006500 $ Carbon

48000.50c -0.0000010 $ Cadmium

3006.66c -0.00000104 $ * Lithium as m7 0.0000000092035

3007.66c -0.00001496 $ * Lithium as m7 0.0000000092035

26000.55c -0.0007250 $ Iron

28000.50c -0.0004500 $ Nickel

4009.66c -0.00000005 $ beryllium

7014.62c -0.0000200 $ * Nitrogen

12000.62c -0.0000100 $ *Magnesuim

20000.62c -0.0000200 $ Calcium

64000.35c -0.00000025 $ Gadolinium element - JRL 6/16/09APENDIX B

APPENDIX C

SAMPLE PLTEMP/ANL INPUT DECK FOR 30 KW POWER SIMULATION.

GHARR-1, 12 Fuel Type, 344 Fuel Rods Model, Radial Geometry, Natural Circulation

Card 100

!2345678901234567890123456789012345678901234567890123456789012345678901234567890

34567890

! MODELING ASSUMPTIONS:

! Each fuel rod is modeled as a FUEL TUBE having a hole of radius 0.0001 mm

! in the center.

! CHECK THE INLET & EXIT LOSS COEFFICIENTS. They are currently calibrated

! to give the measured coolant temp rise of 13 C during natral circulation

! at a power of 15 kW.

! YOU MUST INPUT AXIAL POWER SHAPE LATER. Uniform assumed now.

! Fuel Tube radii: Ra=0 mm, Rb=0.6 mm, Rc=2.15 mm, Rd=2.75 mm, Rwater=6.216743

mm

! Power per fuel rod=30/344=0.08721 kW, Fueled Length=0.230 m, Inlet Temp=30 C

! HydDia = 4*33594.2284/(Pi*5.5*350 + Pi*231) = 19.83929 mm

! Channel Width = Pi*(Rd + Rwater) = Pi*(2.75 + 6.216743) = 28.16985 mm

! Channel Thickness = Rwater - Rd = 6.216743 - 2.75 = 3.466743 mm

! Chimney Height = Dist from fuel rod upper end to bottom of Aluminum Shim=16 mm

! Fuel Plate Width = Pi*(Rb + Rc) = Pi*(0.6 + 2.15) = 8.63938 mm

! 1 2 3 4 5 6 7 8 9 10 11 12 13 14 15 16 17 18 19 20

51 0 6 12 0 0 1 1 1 0 0 0 0 0 0 1 0 0 0 1 Card 200

```
  1                                                    Card 200A
!       1.0       1.0       1.0                       Card 201
 30   3      0.005       1.0       1.0       1.0   0   0          Card 300
!       1.0       1.0       1.0                       Card 300A
  1   2       1.0                                     Card 301
  1   1   1                                           Card 302
      1.352     1.352     1.352     1.352     1.352     1.352     Card 303
      1.352     1.352     1.352     1.352     1.352     1.352     Card 303
      1.352     1.352     1.352     1.352     1.352     1.352     Card 303
      1.352     1.352     1.352     1.352     1.352     1.352     Card 303
      1.352     1.352     1.352     1.352     1.352     1.352     Card 303
 9.765764E-5 1.983929E-2      0.009      64.0 28.16985E-3 3.466743E-3      Card 304
 9.765764E-5 1.983929E-2      0.230       0.0 28.16985E-3 3.466743E-3      Card 304
 9.765764E-5 1.983929E-2      0.009      64.0 28.16985E-3 3.466743E-3      Card 304
      0.0       0.0       0.0       0.016                 Card 305
  2   0       0.0       0.230   0.5999E-3     180.0      1.55E-3     160.0   Card 306
 9.765764E-7 1.983929E-2 17.27876E-3 17.27876E-3 28.16985E-3 3.466743E-3
Card 307
 9.765764E-5 1.983929E-2 17.27876E-3 17.27876E-3 28.16985E-3 3.466743E-3
Card 307
  8.63938E-3                                          Card 308
   1.375E-3                                           Card 308A
     1.193                                            Card 309
```

1.347	Card 309
1.481	Card 309
1.576	Card 309
1.627	Card 309
1.631	Card 309
1.588	Card 309
1.498	Card 309
1.363	Card 309
2.212	Card 309
1.193	Card 309
1.347	Card 309
1.481	Card 309
1.576	Card 309
1.627	Card 309
1.631	Card 309
1.588	Card 309
1.498	Card 309
1.363	Card 309
2.212	Card 309
1.193	Card 309
1.347	Card 309
1.481	Card 309
1.576	Card 309

1.627 Card 309

1.631 Card 309

1.588 Card 309

1.498 Card 309

1.363 Card 309

2.212 Card 309

30 3 0.005 1.0 1.0 1.0 0 0 Card 300

! 1.0 1.0 1.0 Card 300A

1 2 1.0 Card 301

1 1 1 Card 302

1.352 1.352 1.352 1.352 1.352 1.352 Card 303

1.352 1.352 1.352 1.352 1.352 1.352 Card 303

1.352 1.352 1.352 1.352 1.352 1.352 Card 303

1.352 1.352 1.352 1.352 1.352 1.352 Card 303

1.352 1.352 1.352 1.352 1.352 1.352 Card 303

9.765764E-5 1.983929E-2 0.009 64.0 28.16985E-3 3.466743E-3 Card 304

9.765764E-5 1.983929E-2 0.230 0.0 28.16985E-3 3.466743E-3 Card 304

9.765764E-5 1.983929E-2 0.009 64.0 28.16985E-3 3.466743E-3 Card 304

0.0 0.0 0.0 0.016 Card 305

2 0 0.0 0.230 0.5999E-3 180.0 1.55E-3 160.0 Card 306

9.765764E-7 1.983929E-2 17.27876E-3 17.27876E-3 28.16985E-3 3.466743E-3

Card 307

9.765764E-5 1.983929E-2 17.27876E-3 17.27876E-3 28.16985E-3 3.466743E-3

Card 307

8.63938E-3 Card 308

1.375E-3 Card 308A

1.193 Card 309

1.347 Card 309

1.481 Card 309

1.576 Card 309

1.627 Card 309

1.631 Card 309

1.588 Card 309

1.498 Card 309

1.363 Card 309

2.212 Card 309

1.193 Card 309

1.347 Card 309

1.481 Card 309

1.576 Card 309

1.627 Card 309

1.631 Card 309

1.588 Card 309

1.498 Card 309

1.363 Card 309

2.212 Card 309

1.193 Card 309

1.347 Card 309

1.481 Card 309

1.576 Card 309

1.627 Card 309

1.631 Card 309

1.588 Card 309

1.498 Card 309

1.363 Card 309

2.212 Card 309

30 3 0.005 1.0 1.0 1.0 0 0 Card 300

! 1.0 1.0 1.0 Card 300A

1 2 1.0 Card 301

1 1 1 Card 302

1.352 1.352 1.352 1.352 1.352 1.352 Card 303

1.352 1.352 1.352 1.352 1.352 1.352 Card 303

1.352 1.352 1.352 1.352 1.352 1.352 Card 303

1.352 1.352 1.352 1.352 1.352 1.352 Card 303

1.352 1.352 1.352 1.352 1.352 1.352 Card 303

9.765764E-5 1.983929E-2 0.009 64.0 28.16985E-3 3.466743E-3 Card 304

9.765764E-5 1.983929E-2 0.230 0.0 28.16985E-3 3.466743E-3 Card 304

9.765764E-5 1.983929E-2 0.009 64.0 28.16985E-3 3.466743E-3 Card 304

0.0 0.0 0.0 0.016 Card 305

2 0 0.0 0.230 0.5999E-3 180.0 1.55E-3 160.0 Card 306

9.765764E-7 1.983929E-2 17.27876E-3 17.27876E-3 28.16985E-3 3.466743E-3

Card 307

9.765764E-5 1.983929E-2 17.27876E-3 17.27876E-3 28.16985E-3 3.466743E-3

Card 307

8.63938E-3 Card 308

1.375E-3 Card 308A

1.193 Card 309

1.347 Card 309

1.481 Card 309

1.576 Card 309

1.627 Card 309

1.631 Card 309

1.588 Card 309

1.498 Card 309

1.363 Card 309

2.212 Card 309

1.193 Card 309

1.347 Card 309

1.481 Card 309

1.576 Card 309

1.627 Card 309

1.631 Card 309

1.588 Card 309

1.498 Card 309

1.363 Card 309

2.212 Card 309

1.193 Card 309

1.347 Card 309

1.481 Card 309

1.576 Card 309

1.627 Card 309

1.631 Card 309

1.588 Card 309

1.498 Card 309

1.363 Card 309

2.212 Card 309

30 3 0.005 1.0 1.0 1.0 0 0 Card 300

! 1.0 1.0 1.0 Card 300A

1 2 1.0 Card 301

1 1 1 Card 302

1.352 1.352 1.352 1.352 1.352 1.352 Card 303

1.352 1.352 1.352 1.352 1.352 1.352 Card 303

1.352 1.352 1.352 1.352 1.352 1.352 Card 303

1.352 1.352 1.352 1.352 1.352 1.352 Card 303

1.352 1.352 1.352 1.352 1.352 1.352 Card 303

9.765764E-5 1.983929E-2 0.009 64.0 28.16985E-3 3.466743E-3 Card 304

9.765764E-5 1.983929E-2 0.230 0.0 28.16985E-3 3.466743E-3 Card 304

9.765764E-5 1.983929E-2 0.009 64.0 28.16985E-3 3.466743E-3 Card 304

0.0 0.0 0.0 0.016 Card 305

2 0 0.0 0.230 0.5999E-3 180.0 1.55E-3 160.0 Card 306

9.765764E-7 1.983929E-2 17.27876E-3 17.27876E-3 28.16985E-3 3.466743E-3 Card 307

9.765764E-5 1.983929E-2 17.27876E-3 17.27876E-3 28.16985E-3 3.466743E-3 Card 307

8.63938E-3 Card 308

1.375E-3 Card 308A

1.193 Card 309

1.347 Card 309

1.481 Card 309

1.576 Card 309

1.627 Card 309

1.631 Card 309

1.588 Card 309

1.498 Card 309

1.363 Card 309

2.212 Card 309

1.193 Card 309

1.347 Card 309

1.481 Card 309

1.576 Card 309

1.627 Card 309

1.631 Card 309

1.588 Card 309

1.498 Card 309

1.363 Card 309

2.212 Card 309

1.193 Card 309

1.347 Card 309

1.481 Card 309

1.576 Card 309

1.627 Card 309

1.631 Card 309

1.588 Card 309

1.498 Card 309

1.363 Card 309

2.212 Card 309

30 3 0.005 1.0 1.0 1.0 0 0 Card 300

! 1.0 1.0 1.0 Card 300A

1 2 1.0 Card 301

1 1 1 Card 302

1.352 1.352 1.352 1.352 1.352 1.352 Card 303

1.352 1.352 1.352 1.352 1.352 1.352 Card 303

1.352 1.352 1.352 1.352 1.352 1.352 Card 303

1.352 1.352 1.352 1.352 1.352 1.352 Card 303

1.352 1.352 1.352 1.352 1.352 1.352 Card 303

9.765764E-5 1.983929E-2 0.009 64.0 28.16985E-3 3.466743E-3 Card 304

9.765764E-5 1.983929E-2 0.230 0.0 28.16985E-3 3.466743E-3 Card 304

9.765764E-5 1.983929E-2 0.009 64.0 28.16985E-3 3.466743E-3 Card 304

0.0 0.0 0.0 0.016 Card 305

2 0 0.0 0.230 0.5999E-3 180.0 1.55E-3 160.0 Card 306

9.765764E-7 1.983929E-2 17.27876E-3 17.27876E-3 28.16985E-3 3.466743E-3
Card 307

9.765764E-5 1.983929E-2 17.27876E-3 17.27876E-3 28.16985E-3 3.466743E-3
Card 307

8.63938E-3 Card 308

1.375E-3 Card 308A

1.193 Card 309

1.347 Card 309

1.481 Card 309

1.576 Card 309

1.627 Card 309

1.631 Card 309

1.588 Card 309

1.498	Card 309
1.363	Card 309
2.212	Card 309
1.193	Card 309
1.347	Card 309
1.481	Card 309
1.576	Card 309
1.627	Card 309
1.631	Card 309
1.588	Card 309
1.498	Card 309
1.363	Card 309
2.212	Card 309
1.193	Card 309
1.347	Card 309
1.481	Card 309
1.576	Card 309
1.627	Card 309
1.631	Card 309
1.588	Card 309
1.498	Card 309
1.363	Card 309
2.212	Card 309

```
 30   3      0.005       1.0       1.0       1.0   0   0            Card 300
!      1.0       1.0       1.0                                    Card 300A
  1   2       1.0                                                  Card 301
  1   1   1                                                        Card 302
      1.352     1.352     1.352     1.352     1.352     1.352     Card 303
      1.352     1.352     1.352     1.352     1.352     1.352     Card 303
      1.352     1.352     1.352     1.352     1.352     1.352     Card 303
      1.352     1.352     1.352     1.352     1.352     1.352     Card 303
      1.352     1.352     1.352     1.352     1.352     1.352     Card 303
 9.765764E-5 1.983929E-2      0.009      64.0 28.16985E-3 3.466743E-3      Card 304
 9.765764E-5 1.983929E-2      0.230       0.0 28.16985E-3 3.466743E-3      Card 304
 9.765764E-5 1.983929E-2      0.009      64.0 28.16985E-3 3.466743E-3      Card 304
       0.0       0.0       0.0       0.016                          Card 305
  2   0       0.0       0.230   0.5999E-3    180.0      1.55E-3    160.0   Card 306
 9.765764E-7 1.983929E-2 17.27876E-3 17.27876E-3 28.16985E-3 3.466743E-3
Card 307
 9.765764E-5 1.983929E-2 17.27876E-3 17.27876E-3 28.16985E-3 3.466743E-3
Card 307
  8.63938E-3                                                       Card 308
    1.375E-3                                                       Card 308A
      1.193                                                        Card 309
      1.347                                                        Card 309
      1.481                                                        Card 309
```

1.576	Card 309
1.627	Card 309
1.631	Card 309
1.588	Card 309
1.498	Card 309
1.363	Card 309
2.212	Card 309
1.193	Card 309
1.347	Card 309
1.481	Card 309
1.576	Card 309
1.627	Card 309
1.631	Card 309
1.588	Card 309
1.498	Card 309
1.363	Card 309
2.212	Card 309
1.193	Card 309
1.347	Card 309
1.481	Card 309
1.576	Card 309
1.627	Card 309
1.631	Card 309

1.588 Card 309

1.498 Card 309

1.363 Card 309

2.212 Card 309

30 3 0.005 1.0 1.0 1.0 0 0 Card 300

! 1.0 1.0 1.0 Card 300A

1 2 1.0 Card 301

1 1 1 Card 302

1.352 1.352 1.352 1.352 1.352 1.352 Card 303

1.352 1.352 1.352 1.352 1.352 1.352 Card 303

1.352 1.352 1.352 1.352 1.352 1.352 Card 303

1.352 1.352 1.352 1.352 1.352 1.352 Card 303

1.352 1.352 1.352 1.352 1.352 1.352 Card 303

9.765764E-5 1.983929E-2 0.009 64.0 28.16985E-3 3.466743E-3 Card 304

9.765764E-5 1.983929E-2 0.230 0.0 28.16985E-3 3.466743E-3 Card 304

9.765764E-5 1.983929E-2 0.009 64.0 28.16985E-3 3.466743E-3 Card 304

0.0 0.0 0.0 0.016 Card 305

2 0 0.0 0.230 0.5999E-3 180.0 1.55E-3 160.0 Card 306

9.765764E-7 1.983929E-2 17.27876E-3 17.27876E-3 28.16985E-3 3.466743E-3 Card 307

9.765764E-5 1.983929E-2 17.27876E-3 17.27876E-3 28.16985E-3 3.466743E-3 Card 307

8.63938E-3 Card 308

1.375E-3	Card 308A
1.193	Card 309
1.347	Card 309
1.481	Card 309
1.576	Card 309
1.627	Card 309
1.631	Card 309
1.588	Card 309
1.498	Card 309
1.363	Card 309
2.212	Card 309
1.193	Card 309
1.347	Card 309
1.481	Card 309
1.576	Card 309
1.627	Card 309
1.631	Card 309
1.588	Card 309
1.498	Card 309
1.363	Card 309
2.212	Card 309
1.193	Card 309
1.347	Card 309

```
      1.481                                                    Card 309
      1.576                                                    Card 309
      1.627                                                    Card 309
      1.631                                                    Card 309
      1.588                                                    Card 309
      1.498                                                    Card 309
      1.363                                                    Card 309
      2.212                                                    Card 309
 30   3      0.005      1.0       1.0       1.0    0   0          Card 300
!      1.0       1.0       1.0                                  Card 300A
 1    2       1.0                                               Card 301
 1    1   1                                                     Card 302
      1.352     1.352     1.352     1.352     1.352     1.352    Card 303
      1.352     1.352     1.352     1.352     1.352     1.352    Card 303
      1.352     1.352     1.352     1.352     1.352     1.352    Card 303
      1.352     1.352     1.352     1.352     1.352     1.352    Card 303
      1.352     1.352     1.352     1.352     1.352     1.352    Card 303
9.765764E-5 1.983929E-2     0.009      64.0 28.16985E-3 3.466743E-3    Card 304
9.765764E-5 1.983929E-2     0.230       0.0 28.16985E-3 3.466743E-3    Card 304
9.765764E-5 1.983929E-2     0.009      64.0 28.16985E-3 3.466743E-3    Card 304
       0.0       0.0       0.0       0.016                    Card 305
 2    0       0.0       0.230   0.5999E-3     180.0      1.55E-3     160.0   Card 306
```

9.765764E-7 1.983929E-2 17.27876E-3 17.27876E-3 28.16985E-3 3.466743E-3

Card 307

9.765764E-5 1.983929E-2 17.27876E-3 17.27876E-3 28.16985E-3 3.466743E-3

Card 307

8.63938E-3 Card 308

1.375E-3 Card 308A

1.193 Card 309

1.347 Card 309

1.481 Card 309

1.576 Card 309

1.627 Card 309

1.631 Card 309

1.588 Card 309

1.498 Card 309

1.363 Card 309

2.212 Card 309

1.193 Card 309

1.347 Card 309

1.481 Card 309

1.576 Card 309

1.627 Card 309

1.631 Card 309

1.588 Card 309

1.498 Card 309

1.363 Card 309

2.212 Card 309

1.193 Card 309

1.347 Card 309

1.481 Card 309

1.576 Card 309

1.627 Card 309

1.631 Card 309

1.588 Card 309

1.498 Card 309

1.363 Card 309

2.212 Card 309

30 3 0.005 1.0 1.0 1.0 0 0 Card 300

! 1.0 1.0 1.0 Card 300A

1 2 1.0 Card 301

1 1 1 Card 302

1.352 1.352 1.352 1.352 1.352 1.352 Card 303

1.352 1.352 1.352 1.352 1.352 1.352 Card 303

1.352 1.352 1.352 1.352 1.352 1.352 Card 303

1.352 1.352 1.352 1.352 1.352 1.352 Card 303

1.352 1.352 1.352 1.352 1.352 1.352 Card 303

9.765764E-5 1.983929E-2 0.009 64.0 28.16985E-3 3.466743E-3 Card 304

9.765764E-5 1.983929E-2 0.230 0.0 28.16985E-3 3.466743E-3 Card 304

9.765764E-5 1.983929E-2 0.009 64.0 28.16985E-3 3.466743E-3 Card 304

0.0 0.0 0.0 0.016 Card 305

2 0 0.0 0.230 0.5999E-3 180.0 1.55E-3 160.0 Card 306

9.765764E-7 1.983929E-2 17.27876E-3 17.27876E-3 28.16985E-3 3.466743E-3 Card 307

9.765764E-5 1.983929E-2 17.27876E-3 17.27876E-3 28.16985E-3 3.466743E-3 Card 307

8.63938E-3 Card 308

1.375E-3 Card 308A

1.193 Card 309

1.347 Card 309

1.481 Card 309

1.576 Card 309

1.627 Card 309

1.631 Card 309

1.588 Card 309

1.498 Card 309

1.363 Card 309

2.212 Card 309

1.193 Card 309

1.347 Card 309

1.481 Card 309

1.576 Card 309

1.627 Card 309

1.631 Card 309

1.588 Card 309

1.498 Card 309

1.363 Card 309

2.212 Card 309

1.193 Card 309

1.347 Card 309

1.481 Card 309

1.576 Card 309

1.627 Card 309

1.631 Card 309

1.588 Card 309

1.498 Card 309

1.363 Card 309

2.212 Card 309

30 3 0.005 1.0 1.0 1.0 0 0 Card 300

! 1.0 1.0 1.0 Card 300A

1 2 1.0 Card 301

1 1 1 Card 302

1.352 1.352 1.352 1.352 1.352 1.352 Card 303

1.352 1.352 1.352 1.352 1.352 1.352 Card 303

1.352 1.352 1.352 1.352 1.352 1.352 Card 303

1.352 1.352 1.352 1.352 1.352 1.352 Card 303

1.352 1.352 1.352 1.352 1.352 1.352 Card 303

9.765764E-5 1.983929E-2 0.009 64.0 28.16985E-3 3.466743E-3 Card 304

9.765764E-5 1.983929E-2 0.230 0.0 28.16985E-3 3.466743E-3 Card 304

9.765764E-5 1.983929E-2 0.009 64.0 28.16985E-3 3.466743E-3 Card 304

0.0 0.0 0.0 0.016 Card 305

2 0 0.0 0.230 0.5999E-3 180.0 1.55E-3 160.0 Card 306

9.765764E-7 1.983929E-2 17.27876E-3 17.27876E-3 28.16985E-3 3.466743E-3

Card 307

9.765764E-5 1.983929E-2 17.27876E-3 17.27876E-3 28.16985E-3 3.466743E-3

Card 307

8.63938E-3 Card 308

1.375E-3 Card 308A

1.193 Card 309

1.347 Card 309

1.481 Card 309

1.576 Card 309

1.627 Card 309

1.631 Card 309

1.588 Card 309

1.498 Card 309

1.363 Card 309

2.212 Card 309

1.193 Card 309

1.347 Card 309

1.481 Card 309

1.576 Card 309

1.627 Card 309

1.631 Card 309

1.588 Card 309

1.498 Card 309

1.363 Card 309

2.212 Card 309

1.193 Card 309

1.347 Card 309

1.481 Card 309

1.576 Card 309

1.627 Card 309

1.631 Card 309

1.588 Card 309

1.498 Card 309

1.363 Card 309

2.212 Card 309

30 3 0.005 1.0 1.0 1.0 0 0 Card 300

! 1.0 1.0 1.0 Card 300A

```
1   2       1.0                                                     Card 301
1   1   1                                                           Card 302
    1.352   1.352   1.352   1.352   1.352   1.352   Card 303
    1.352   1.352   1.352   1.352   1.352   1.352   Card 303
    1.352   1.352   1.352   1.352   1.352   1.352   Card 303
    1.352   1.352   1.352   1.352   1.352   1.352   Card 303
    1.352   1.352   1.352   1.352   1.352   1.352   Card 303
9.765764E-5 1.983929E-2     0.009     64.0 28.16985E-3 3.466743E-3     Card 304
9.765764E-5 1.983929E-2     0.230      0.0 28.16985E-3 3.466743E-3     Card 304
9.765764E-5 1.983929E-2     0.009     64.0 28.16985E-3 3.466743E-3     Card 304
    0.0     0.0     0.0     0.016                   Card 305
2   0       0.0     0.230   0.5999E-3   180.0     1.55E-3   160.0   Card 306
9.765764E-7 1.983929E-2 17.27876E-3 17.27876E-3 28.16985E-3 3.466743E-3
Card 307
9.765764E-5 1.983929E-2 17.27876E-3 17.27876E-3 28.16985E-3 3.466743E-3
Card 307
 8.63938E-3                                                     Card 308
  1.375E-3                                                      Card 308A
    1.193                                                       Card 309
    1.347                                                       Card 309
    1.481                                                       Card 309
    1.576                                                       Card 309
    1.627                                                       Card 309
```

1.631	Card 309
1.588	Card 309
1.498	Card 309
1.363	Card 309
2.212	Card 309
1.193	Card 309
1.347	Card 309
1.481	Card 309
1.576	Card 309
1.627	Card 309
1.631	Card 309
1.588	Card 309
1.498	Card 309
1.363	Card 309
2.212	Card 309
1.193	Card 309
1.347	Card 309
1.481	Card 309
1.576	Card 309
1.627	Card 309
1.631	Card 309
1.588	Card 309
1.498	Card 309

1.363 Card 309

2.212 Card 309

14 3 0.005 1.0 1.0 1.0 0 0 Card 300

! 1.0 1.0 1.0 Card 300A

1 2 1.0 Card 301

1 1 1 Card 302

1.352 1.352 1.352 1.352 1.352 1.352 Card 303

1.352 1.352 1.352 1.352 1.352 1.352 Card 303

1.352 1.352 Card 303

9.765764E-5 1.983929E-2 0.009 64.0 28.16985E-3 3.466743E-3 Card 304

9.765764E-5 1.983929E-2 0.230 0.0 28.16985E-3 3.466743E-3 Card 304

9.765764E-5 1.983929E-2 0.009 64.0 28.16985E-3 3.466743E-3 Card 304

0.0 0.0 0.0 0.016 Card 305

2 0 0.0 0.230 0.5999E-3 180.0 1.55E-3 160.0 Card 306

9.765764E-7 1.983929E-2 17.27876E-3 17.27876E-3 28.16985E-3 3.466743E-3

Card 307

9.765764E-5 1.983929E-2 17.27876E-3 17.27876E-3 28.16985E-3 3.466743E-3

Card 307

8.63938E-3 Card 308

1.375E-3 Card 308A

1.193 Card 309

1.347 Card 309

1.481 Card 309

```
      1.576                                                Card 309
      1.627                                                Card 309
      1.631                                                Card 309
      1.588                                                Card 309
      1.498                                                Card 309
      1.363                                                Card 309
      2.212                                                Card 309
      1.193                                                Card 309
      1.347                                                Card 309
      1.481                                                Card 309
      1.576                                                Card 309
!                          POWER    TIN      PRESS
! Power in 6 fuel rods =30/344*344 = 30.00000kW at a reactor power of 30 kW.
    8.0E-6     0.040     0.000 3.000000E-2 24.5     0.172370        Card 500
      0.0       0.0       0.80      0.02                 Card 500
 50    1.0E-4     32.5      0.00      0.00                 Card 600
 21                                                      Card 700
0.0       1.189                                         Card 701
0.100     1.117                                         Card 701
0.148     1.130                                         Card 701
0.196     1.169                                         Card 701
0.244     1.202                                         Card 701
0.292     1.248                                         Card 701
```

0.340	1.291	Card 701
0.388	1.318	Card 701
0.436	1.324	Card 701
0.484	1.332	Card 701
0.532	1.352	Card 701
0.580	1.311	Card 701
0.628	1.285	Card 701
0.676	1.260	Card 701
0.724	1.205	Card 701
0.772	1.152	Card 701
0.820	1.108	Card 701
0.868	1.036	Card 701
0.916	0.982	Card 701
0.964	0.972	Card 701
1.000	1.069	Card 701
0		Card 702

APPENDIX D

SAMPLE INPUT DECK FOR PARET/ANL CODE FOR 2.1 MK REACTIVITY INSERTION

```
    0
* PARET:  GHARR1   HEU  2 CHAN  2.1 mk transient
! inlet and exit K-factors of 80.
!  react.aug02.ciae.k80.inp
!      NCHN    NZ   NR IGEOM IPROP IRXSWT
1001,    -2   21   7    1    1    1
1002,     0    0   6   -1    0   20
! assuming 4.3 mm meat od, 0.6mm clad thickness, 344 rods
! active length 0.23 m
!xxxxx11111111111122222222222333333333333444444444444555555555555666666
666666
!       POWER, MW                    ENTHIN       RS
1003,     2.00-6 0.001159002   1.72370+5  -24.50     2.7502002-3
!       RF         RC                        AL        ALDDIN
1004,    2.15000-3   2.15020-3   0.0        0.0        0.2300     0.000
!       ALDDEX       beta
1005,    0.016     0.008175071   8.14700-5   9.80664     0.002994
!       TRANST                      rho (20C)    GAMMA0
1006,    1000.      0.80        1.0       996.88       0.0
!       GAMMA1      GAMMA2      GAMMA3      GAMMA4      DOPPN       EPS3
```

1007, 4.00000-5 -2.4-8 4.0-10 -4.5-14 1.00 0.001

! DNBQDP TAUUNB TAUUTB ALAMNB ALAMTB ALAMFB

1008, 0.00 0.001 0.001 0.05 0.05 0.05

! HTTCON HTTEXP

!1009, 1.4 0.33

! try using 0.92 to reduce h

1009, 0.923 0.33

! PSUBC

1111, 0.033370 1.00 1.00

! IMODE IHT

! use CIAE option

1112, 3 1 0 1 0 0

! RDRATE TDLAY POWTP FLOTP OPT POW0

1113, 1.016 0.015 10000.0 0.0 0. 0.0

! HNCTOP HNCBOT FOR NATURAL CONVECTION:HEIGHT ABOVE AND BELOW CORE

!xxxxx1111111111112222222222223333333333334444444444455555555555566666666666

1114, 0.0160 0.0150 2300. 6000.0 1. 1.6

! fuel k; then fuel rho*cp

! per Floyd July 31/07

2001, 0.0 0.0 167.6 0.00 0.00

2002, 0.0 0.0000+0 2.2400+6 0.00 0.00

! air gap per Floyd July 31/07

2003, 0.0 0.000000 0.0282 0.00 0.00

2004, 0.0 0.0000 1.02000+4 0.00 0.00

! Aluminum clad;

! per Floyd July 31/07

2005, 0.0 0.0 199.7 0.00 0.00

2006, 0.0 0.0000 2.420+6 0.00 0.00

! radial data: 4.3 mm od meat; 0.6 mm clad;

3001, 0.537500-3 5 1 1.000

! minute gap per Floyd 8/1/07

3002, 0.000200-3 6 2 0.00

3003, 0.600000-3 7 3 0.000

4001, 10.9524E-3 21

!xxxxx1111111111112222222222233333333333344444444444455555555555566666666666

! RN BM ALOSCN ALOSCX

5100, 4 1. 0.006206 0.0189848 80. 80.

! SIGIN SIGEX DVOID DTMP

5100, 7.66 6.57 -0.01864 7.2-4

5101, 0.0000 0.0000 1.2412-2 1.2412-2

5102, 1.1889 1.00 1.00 1.00

5103, 1.1169 1.00 1.00 1.00

5104, 1.1296 1.00 1.00 1.00

5105, 1.1690 1.00 1.00 1.00

5106, 1.2023 1.00 1.00 1.00

5107, 1.2476 1.00 1.00 1.00

5108, 1.2913 1.00 1.00 1.00

5109, 1.3183 1.00 1.00 1.00

5110, 1.3243 1.00 1.00 1.00

5111, 1.3316 1.00 1.00 1.00

5112, 1.3522 1.00 1.00 1.00

5113, 1.3115 1.00 1.00 1.00

5114, 1.2851 1.00 1.00 1.00

5115, 1.2603 1.00 1.00 1.00

5116, 1.2046 1.00 1.00 1.00

5117, 1.1525 1.00 1.00 1.00

5118, 1.1076 1.00 1.00 1.00

5119, 1.0364 1.00 1.00 1.00

5120, 0.9820 1.00 1.00 1.00

5121, 0.9725 1.00 1.00 1.00

5122, 1.0695 1.00 1.00 1.00

!xxxxx1111111111112222222222223333333333334444444444445555555555566666666

666666

5200, 4 1. 0.006206 0.9810152 80. 80.

5200, 7.66 6.57 1.0 1.0

5201, 0.0000 0.0000 1.2412-2 1.2412-2

5202, 1.0049 1.00 1.00 1.00

5203, 0.9303 1.00 1.00 1.00

5204, 0.9410 1.00 1.00 1.00

5205, 0.9752 1.00 1.00 1.00

5206, 1.0127 1.00 1.00 1.00

5207, 1.0483 1.00 1.00 1.00

5208, 1.0766 1.00 1.00 1.00

5209, 1.0986 1.00 1.00 1.00

5210, 1.1130 1.00 1.00 1.00

5211, 1.1188 1.00 1.00 1.00

5212, 1.1150 1.00 1.00 1.00

5213, 1.1035 1.00 1.00 1.00

5214, 1.0816 1.00 1.00 1.00

5215, 1.0522 1.00 1.00 1.00

5216, 1.0139 1.00 1.00 1.00

5217, 0.9683 1.00 1.00 1.00

5218, 0.9177 1.00 1.00 1.00

5219, 0.8665 1.00 1.00 1.00

5220, 0.8232 1.00 1.00 1.00

5221, 0.8114 1.00 1.00 1.00

5222, 0.9152 1.00 1.00 1.00

6001, 3.79728-2 0.1270-1 0.21299 0.3170-1 0.1880 0.115

6002, 0.40699 0.31100 0.12805 1.4000 2.5981-2 3.8700

```
!xxxxx1111111111112222222222223333333333334444444444455555555555566666666
666666
9000,      4   ! 50 second ramp starting at 70.0 sec
9001,      0.0          0.0
9002,      0.0          70.0
9003,    0.299785      120.0
9004,    0.299785     10000.0
10000,     2
! upflow
! assume some initial flow
!xxxxx1111111111112222222222223333333333334444444444455555555555566666666
666666
10001,   1.000     0.0         1.000    10000.
11000,     2
11001,   0.0       98.0        0.0        2000.0
12000,     2
12001,   0.0       0.0         0.0        0.0
14000,     6
14001,   0.010     0.0
14002,   0.0010    60.0
14003,   0.00010   70.0
14004,   0.0010    400.0
14005,   0.0100    600.0
```

14006, 0.0200 1200.0

16000, 5

!xxxxx1111111111112222222222223333333333334444444444455555555555566666666

666666

16001, 0.1 1000 0.0 5.0 1000 20.0

16002, 1.0 1000 70.0 10.0 500 800.0

16003, 50. 1000 600.0

17000, 11

17001, 1.00 0.0 0.75 2.50 0.50 5.00

17002, 0.25 7.50 0.10 9.00 0.05 9.50

17003, 0.01 9.90 0.005 9.95 0.001 9.99

17004, 0.00 10.00 0.00 30000.

18000, 2

18001, 0.0 0.0 -13.0 0.5080

! coolant feedback with temperature

19000, 6

19001, 5.1733-3 293.00

19002, 8.7515-3 303.15

19003, 7.8180-3 323.15

19004, 8.1972-3 333.15

19005, 8.1972-3 373.15

19006, 8.1972-3 473.15

```
!xxxxx1111111111112222222222223333333333334444444444455555555555566666666
666666
! coolant feedback with void
20000,     6
20001,    0.45888   0.
20002,    0.39202   0.267
20003,    0.39538   1.029
20004,    0.40250   1.513
20005,    0.40250   3.983
20006,    0.0       100.
```

APPENDIX E

PARAMETERS FOR COMMUTING HEAT FLUX AND POWER DENSITY

P = Reactor Power (W)	30,000 /15,000
L_h =Fuel Length (m)	0.230
r_c =Fuel Meat Outer Radius (m)	2.15×10^{-3}
N_f =Number of Active Fuel Rods	344
Wetted Perimeter of Channel 2=Heated Perimeter of Channel	1.72786×10^{-2}
Equation for Power Density in the fuel meat (MW/m^2)	$q''' = \frac{P}{N_f \pi r_c^{\,2} L_h}$